

DYNAMIC BUCKLING OF VISCOPLASTIC SPHERICAL  
SHELLS

Robert Lincoln Dickey

DUDLEY KNOX LIBRARY  
NAVAL POSTGRADUATE SCHOOL  
MONTEREY, CALIFORNIA 93940

DYNAMIC BUCKLING OF  
VISCOPLASTIC SPHERICAL SHELLS

by

LIEUTENANT COMMANDER ROBERT LINCOLN DICKEY, USN  
B.C.E. Rensselaer Polytechnic Institute  
1965

SUBMITTED IN PARTIAL FULFILLMENT  
OF THE REQUIREMENTS FOR THE  
DEGREE OF  
OCEAN ENGINEER  
AND FOR THE DEGREE OF  
MASTER OF SCIENCE IN NAVAL ARCHITECTURE  
AND MARINE ENGINEERING  
AT THE  
MASSACHUSETTS INSTITUTE OF TECHNOLOGY  
MAY 1974



# Dynamic Buckling of Viscoplastic Spherical Shells

by

Lieutenant Commander Robert Lincoln Dickey, USN

Submitted to the Department of Ocean Engineering on May 10, 1974, in partial fulfillment of the requirements for the Degree of Ocean Engineer and for the Degree of Master of Science in Naval Architecture and Marine Engineering.

## Abstract

Buckling is a significant cause of structural failure. A theoretical investigation has been undertaken into the dynamic instability of complete spherical shells which are loaded impulsively and made from a viscoplastic material.

The critical mode numbers obtained in this thesis are similar to those obtained for cylindrical shells having the same  $R/h$  ratios and material parameters while the threshold velocities were for higher viscoplastic spherical shells than for rigid-plastic spherical shells.

Thesis Supervisor: Norman Jones

Title: Associate Professor of Ocean Engineering



### Acknowledgments

The author is grateful for the assistance of Professor Jones and his continuing support, advice and instruction during the preparation of this thesis. Appreciation is also expressed to Professor Alan Needleman and Himangshu Bhattacharya for their advice in obtaining verification of the author's computer program.

Many thanks to Miss Cheryl Gibson for having to put up with very poor handwriting in order to type this thesis.

Lastly, special thanks to my wife Patty, and two children for being so understanding and patient these past months.





## Table of Contents

	<u>Page</u>
Abstract	2
Acknowledgements	3
Table of Contents	4
List of Tables	5
List of Figures	6
List of Symbols	7
Chapter 1: Introduction	10
Chapter 2: Basic Equations	12
Chapter 3: Static Behavior	19
Chapter 4: Dynamic Buckling	21
4.1 Dominant Equation	21
4.2 Perturbation Equation	23
Chapter 5: Results and Discussion	27
Chapter 6: Conclusions	42
Chapter 7: Recommendations	43
References	44
Appendix A: Constitutive Equations of Viscoplastic Spherical Shells	46
Appendix B: Variations of $\gamma$ and $\sigma_0$	51
Appendix C: Computer Program Using Florence Method	54
Appendix D: Computer Program Using Numerical Method	64
Appendix E: Critical Impulse	68



# List of Tables

		<u>Page</u>
Table 1	Critical Mode Numbers for a Viscoplastic Spherical Shell Versus $R/h$ , with $R = 1.460$ in., $V_0 = 9357.6$ in/sec, $\gamma = 6500 \text{ sec}^{-1}$ , $\sigma_0 = 46000$ psi and $\rho = 0.0002523 \text{ lb-sec}^2/\text{in.}^4$ .	27
Table 2	a. A Comparison of the Critical Mode Numbers for a Viscoplastic Spherical Shell with the Corresponding Experimental Results on Cylindrical Shells.	31
	b. Values of $\sigma_0$ , $\rho$ and $\gamma$ that correspond to materials in Table 2a.	34
	c. Values of $\tau_f$ and $C$ that correspond to materials in Table 2a.	35
Table 3	Critical Mode Numbers and Displacement Function Amplitudes Versus Initial Velocities and Differing Values of $\gamma$ with $R = 1.460$ , $R/h = 18.25$ , $\sigma_0 = 46,000$ psi and $\rho = 0.0002523 \text{ lb-sec}^2/\text{in.}^4$ .	39
Table 4	Variation of $\sigma_0/\sigma_e$ and $\Omega_n^{(2)}$ to Various Values of $V_0$ and $\gamma$ with $R = 1.460$ in., $R/h = 18.25$ , $\sigma_0 = 46,000$ psi and $\rho = 0.0002523 \text{ lb-sec}^2/\text{in.}^4$ .	69



## List of Figures

		<u>Page</u>
Figure 1	(a) Displacements and (b) Membrane Forces, Bending Moments and External Loads on a Spherical Shell.	13
Figure 2	Critical Mode of Buckling as a Function of $R/h$ with $V_0 = 9357.58$ in/sec and $\gamma = 6500 \text{ sec}^{-1}$ .*	28
Figure 3	Amplification Functions at $\tau = .2, .4, .6, .8$ , and $1.0 \tau_f$ for (a) Displacement and (b) Velocity Imperfections for a Viscoplastic Spherical Shell with $R = 1.460$ in., $R/h = 18.25$ , and $\gamma = 6500 \text{ sec}^{-1}$ .*	30
Figure 4	Variation of Largest Amplification Function at $\tau = \tau_f$ with Initial Impulsive Velocity for (a) Displacement and (b) Velocity Imperfections for a Viscoplastic Spherical Shell with $R = 1.460$ in., $R/h = 18.25$ , and various values of $\gamma$ . The numbers in parentheses ( ) are the critical modes for $A_{mn}(0)$ and $B_{mn}(0)$ .*	38
Figure 5	Variation of Strain Rate Across Thickness of Section.	50
Figure 6	Cowper and Symonds Power Law and Linear Approximations to it [11].	53

---

\* Figures 2, 3 and 4 all used  $\sigma_0 = 46,000$  psi and  $\rho = .0002523$  lb - sec<sup>2</sup>/in.<sup>4</sup>.



## List of Symbols

$a_{mn}, b_{mn}$	non-dimensional displacement amplitude (15a)
$a_n, b_n$	variable defined in (37e, 37f)
$c_{mn}, d_{mn}$	non-dimensional stress function (15b)
$\dot{e}_{ij}$	membrane strain rate
$h$	thickness of shell
$i, j, m, n$	indices
$k$	yield stress in simple shear $\sigma_0/\sqrt{3}$
$t(t_f)$	time variable (final)
$u$	non-dimensional perturbation displacement $W'/R$
$u_0$	non-dimensional dominant displacement $\bar{W}/R$
$z$	normal coordinate
$A_{mn}$	displacement amplification function
$B_{mn}$	velocity amplification function
$C$	equivalent velocity
$F$	stress function
$\tilde{F}$	non-dimensional stress function
$J_2$	second invariant of the stress deviator
$K$	constant of integration
$M_{ij}$	bending or twisting moment
$M( )$	Kummer function of first kind
$N_{ij}$	resultant membrane stress
$P$	static pressure
$\tilde{P}$	non-dimensional pressure
$Q_n^{(1)}, Q_n^{(2)}$	variables defined (34b, 34c)





$R$	radius of shell
$R_n^2$	variable defined (34d)
$S_{ij}$	deviation stress
$U, V, W$	displacements
$U( )$	Kummer function of second kind
$V_0$	initial velocity
$\alpha^2$	$1/12 (h/R)^2$
$\alpha_n$	non-dimensional radial shell imperfections
$\beta_n$	non-dimensional velocity imperfections
$\beta^2$	$C/(R\gamma^*)$
$\gamma$	viscosity coefficient
$\gamma_1, \gamma^*$	viscosity variables defined (2.5, 1.6d)
$\Gamma$	gamma function
$\delta$	Cowper and Symonds power constant
$\dot{\epsilon}_e (\dot{\epsilon}_e^*)$	equivalent strain rate (initial)
$\dot{\epsilon}_{ij}$	plastic strain rate tensor
$\theta$	circumferential coordinates (angles)
$\kappa_{ij}$	curvature change rates
$\lambda_n$	$n(n + 1)$
$\Lambda_n$	variable defined (37h)
$\mu$	slope of stress-strain rate (2.2)
$\xi$	time variable $1 - \tau/\tau_f$
$\rho$	density of materials
$\sigma_{ij}$	stress tensor
$\sigma_o (\sigma_e, \sigma_{01})$	yield (equivalent, linearized) stress
$\tilde{\sigma}$	non-dimensional stress



$\tau(\tau_f)$	non-dimensional time (terminal)
$\phi$	meridional coordinate
$\tilde{\omega}_n$	variable defined (16b)
$\Omega_n$	variable defined (37g)
$(\dot{\phantom{a}})$	$\frac{\partial}{\partial t}(\phantom{a})$
$(\phantom{a})_{,\tau}$	$\frac{\partial}{\partial \tau}(\phantom{a})$
$\nabla^2(\phantom{a})$	defined (11f)



## Introduction

The analysis of dynamic buckling, of elastic-plastic and rigid plastic cylinders has been investigated by Abrahamson and Goodier [1] extended by Goodier [2], Goodier and Florence [3] and others [4-6]. Florence [7-8] and Wojewodzki [9-11] extended the analysis to viscoplastic cylindrical shells. Work on spherical shells has progressed through elastic-plastic and rigid plastic materials [12-14]. The analytical procedures of the above references were derived by assuming that buckling stemmed from the growth of small imperfections in otherwise uniform initial displacements and velocity fields.

The dynamic buckling of a thin-walled complete spherical shell which is made from a viscoplastic material is investigated herein. A theoretical procedure is developed by first considering the unperturbed motion arising from a spherically symmetric initial velocity field. An examination is then made of the influence of small perturbations in this otherwise uniform velocity field and of the effect of small deviations from the initial sphericity of the shell. It transpires that certain harmonics grow very quickly and cause a spherical shell to exhibit a characteristic wrinkled shape. It is assumed that the strains which are associated with the perturbed state are much smaller than those associated with the predominant motion. Thus, no unloading of the shell material occurs before the time when all the



initial kinetic energy is absorbed by the spherical shell in the predominant mode. Moreover, it is further assumed that the wrinkled pattern in the shells is established prior to this time and is not modified by subsequent unloading.





## Chapter 2

### Basic Equations

The equilibrium equations, compatibility relations and strain and curvature relations have been presented in refs. [13] and [14] for a spherical shell. These results are repeated in this section for convenience.

It may be shown for the particular case of a thin-walled spherical shell that the strain and curvature relations which were developed in reference [12] for an arbitrarily shaped shell, can be written

$$\dot{e}_\phi = \frac{1}{R} (\dot{U}_{,\phi} - \dot{W} + \frac{1}{R} \dot{W}_{,\phi} \dot{W}_{,\phi}) \quad (1a)$$

$$\dot{e}_\theta = \frac{1}{R} (\operatorname{cosec} \phi \dot{V}_{,\theta} + \cot \phi \dot{U} - \dot{W} + \frac{1}{R} \operatorname{cosec}^2 \phi \dot{W}_{,\theta} \dot{W}_{,\theta}) \quad (1b)$$

$$\begin{aligned} \dot{e}_{\phi\theta} = \frac{1}{R} [\operatorname{cosec} \phi \dot{U}_{,\theta} - \cot \phi \dot{V} + \dot{V}_{,\phi} + \\ \frac{1}{R} \operatorname{cosec} \phi (\dot{W}_{,\phi} \dot{W}_{,\theta} + \dot{W}_{,\theta} \dot{W}_{,\phi})] \end{aligned} \quad (1c)$$

$$\dot{\kappa}_\phi = \frac{1}{R^2} (\dot{W} + \dot{W}_{,\phi\phi}) \quad (1d)$$

$$\dot{\kappa}_\theta = \frac{1}{R^2} (\dot{W} + \operatorname{cosec}^2 \phi \dot{W}_{,\theta\theta} + \cot \phi \dot{W}_{,\phi}) \quad (1e)$$

$$\text{and } \dot{\kappa}_{\phi\theta} = \frac{2}{R^2} [\operatorname{cosec} \phi \dot{W}_{,\phi\theta} - \cot \phi \operatorname{cosec} \phi \dot{W}_{,\theta}] \quad (1f)$$

when the displacements are defined as shown in Figure 1. A straightforward modification of the general equations in ref. [12] for a shell of thickness  $h$  and density  $\rho$  gives the equilibrium equations



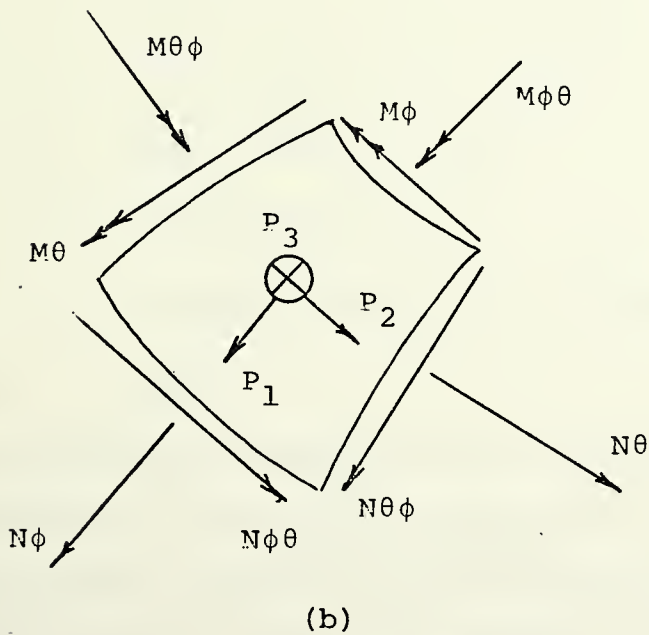
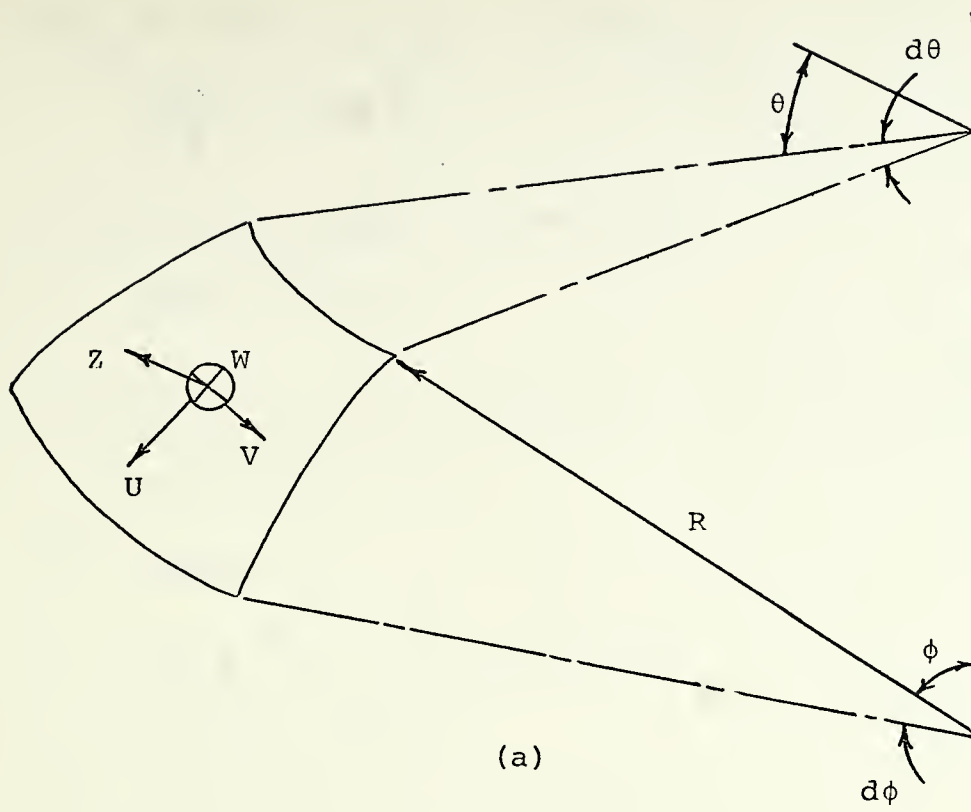


Figure 1: (a) Displacement and (b) Membrane Forces, Bending Moments and External Loads on a Spherical Shell.



$$N_{\phi, \phi} + \cot \phi (N_{\phi} - N_{\theta}) + \operatorname{cosec} \phi N_{\phi \theta, \theta} - \rho h R \ddot{U} + P_1 R = 0 \quad (2a)$$

$$\operatorname{cosec} \phi N_{\theta, \theta} + N_{\phi \theta, \phi} + 2 \cot \phi N_{\phi \theta} - \rho h R \ddot{V} + P_2 R = 0 \quad (2b)$$

and

$$\begin{aligned} R(N_{\phi} + N_{\theta}) + N_{\phi}(W_{, \phi \phi} + \cot \phi W_{, \phi}) + \\ N_{\theta} \operatorname{cosec}^2 \phi W_{, \theta \theta} + \\ \operatorname{cosec} \phi N_{\phi \theta} (W_{, \phi \theta} + W_{, \theta \phi}) + \\ (N_{\phi, \phi} W_{, \phi} + W_{, \theta} N_{\phi \theta, \phi} \operatorname{cosec} \phi + \\ W_{, \phi} N_{\phi \theta, \theta} \operatorname{cosec} \phi + \\ \operatorname{cosec}^2 \phi N_{\theta, \theta} W_{, \theta}) - (M_{\phi, \phi \phi} + \\ 2 \cot \phi M_{\phi, \phi} - \cot \phi M_{\theta, \phi} + \\ 2 M_{\theta} + \operatorname{cosec}^2 \phi M_{\theta, \theta \theta} + \\ 2 \operatorname{cosec} \phi M_{\phi \theta, \phi \theta} + \\ 2 \operatorname{cosec} \phi \cot \phi M_{\phi \theta, \theta}) - R^2 \rho h \ddot{W} + \\ R^2 P_3 = 0 \end{aligned} \quad (2c)$$

which are consistent with equations (1a) and (1f) according to the principle of virtual work provided the influence of transverse shear deformation is disregarded.

The strain and change of curvature relations (1a) to (1f) satisfy the compatibility equation



$$\begin{aligned}
& \dot{e}_{\theta, \phi\phi} + \operatorname{cosec}^2 \phi \dot{e}_{\phi, \theta\theta} + 2 \cot \phi \dot{e}_{\theta, \phi} - \\
& \cot \phi \dot{e}_{\phi, \phi} + 2 \dot{e}_{\phi} - \operatorname{cosec} \phi \dot{e}_{\phi\theta, \phi\theta} - \\
& \operatorname{cosec} \phi \cot \phi \dot{e}_{\phi\theta, \theta} + R(\dot{\kappa}_{\phi} + \dot{\kappa}_{\theta}) = 0
\end{aligned} \tag{3}$$

for infinitesimal displacements [12].

The constitutive equations for spherical shells which are made from rigid viscoplastic material are developed in Appendix A. Equations (1.8a) to (1.8f) for a spherical shell made from rigid viscoplastic material can be written in the form

$$N_{\phi} = \frac{kh}{\gamma^*} (2\dot{e}_{\phi} + \dot{e}_{\theta}) \tag{4a}$$

$$N_{\theta} = \frac{kh}{\gamma^*} (2\dot{e}_{\theta} + \dot{e}_{\phi}) \tag{4b}$$

$$N_{\phi\theta} = \frac{kh}{\gamma^*} \frac{\dot{e}_{\phi\theta}}{2} \tag{4c}$$

$$M_{\phi} = \frac{kh^3}{12\gamma^*} (2\dot{\kappa}_{\phi} + \dot{\kappa}_{\theta}) \tag{4d}$$

$$M_{\theta} = \frac{kh^3}{12\gamma^*} (2\dot{\kappa}_{\theta} + \dot{\kappa}_{\phi}) \tag{4e}$$

$$\text{and } M_{\phi\theta} = \frac{kh^3}{12\gamma^*} \frac{\dot{\kappa}_{\phi\theta}}{2} \tag{4f}$$

$$\text{where } k = \sigma_0 / \sqrt{3} \tag{5a}$$

$$\text{and } \gamma^* = \gamma(1 - k/\sqrt{J_2}). \tag{5b}$$

The method of solution used here is similar to that used in refs. [12] and [13]. It is assumed that the displacement in a complete spherical shell consists of dominant parts





( $\bar{W}$ ,  $\bar{U} = \bar{V} = 0$ ) and perturbation parts ( $w'$ ,  $u'$ ,  $v'$ ) so that

$$W(\phi, \theta, \tau) = \bar{W}(\tau) + W'(\phi, \theta, \tau) \quad (6a)$$

$$U(\phi, \theta, \tau) = U'(\phi, \theta, \tau) \quad (6b)$$

and  $V(\phi, \theta, \tau) = V'(\phi, \theta, \tau).$  (6c)

Thus, the dominant strains and curvature changes are

$$\bar{e}_\phi = \bar{e}_\theta = -\frac{\bar{W}}{R}, \quad \bar{e}_{\phi\theta} = 0. \quad (7a-c)$$

and  $\bar{\kappa}_\phi = \bar{\kappa}_\theta = \frac{\bar{W}}{R^2}, \quad \bar{\kappa}_{\phi\theta} = 0 \quad (7d-f)$

respectively, while the corresponding perturbation quantities are given by equation (1a) to (1f) with primes. Similarly,

$$N_\phi(\phi, \theta, \tau) = \bar{N}(\tau) + N'_\phi(\phi, \theta, \tau) \quad (8a)$$

$$N_\theta(\phi, \theta, \tau) = \bar{N}(\tau) + N'_\theta(\phi, \theta, \tau) \quad (8b)$$

$$N_{\phi\theta}(\phi, \theta, \tau) = N'_{\phi\theta}(\phi, \theta, \tau) \quad (8c)$$

$$M_\phi(\phi, \theta, \tau) = \bar{M}(\tau) + M'_\phi(\phi, \theta, \tau) \quad (8d)$$

$$M_\theta(\phi, \theta, \tau) = \bar{M}(\tau) + M'_\theta(\phi, \theta, \tau) \quad (8e)$$

and  $M_{\phi\theta}(\phi, \theta, \tau) = M'_{\phi\theta}(\phi, \theta, \tau). \quad (8f)$

If equations (6) and (8) are substituted into equation (2c), then the dominant and perturbation transverse equilibrium equations are

$$2 \frac{\bar{N}}{R} - 2 \frac{\bar{M}}{R^2} + P_3 - \rho h \ddot{\bar{W}} = 0 \quad (9a)$$



and

$$\begin{aligned}
& R(N'_{\phi} + N'_{\theta}) + \bar{N}(W'_{,\phi\phi} + \cot\phi W'_{,\phi} + \operatorname{cosec}^2\phi W'_{,\theta\theta}) - \\
& [M'_{\phi,\phi\phi} + 2 \cot\phi M'_{\phi,\phi} - \cot\phi M'_{\theta,\phi} + \\
& 2M'_{\theta} + \operatorname{cosec}^2\phi M'_{\theta,\theta\theta} + 2 \operatorname{cosec}\phi M'_{\phi\theta,\theta\phi} + \\
& 2 \operatorname{cosec}\phi \cot\phi M'_{\phi\theta,\theta}] - \rho h R^2 \ddot{W}' = 0
\end{aligned} \tag{9b}$$

respectively, when neglecting higher order quantities.

It may be shown that in-plane equilibrium equations (2a) and (2b) are satisfied identically when

$$N_{\phi} = \frac{1}{R^2} [F + \operatorname{cosec}^2\phi F_{,\phi\phi} + \cot\phi F_{,\phi}] \tag{10a}$$

$$N_{\theta} = \frac{1}{R^2} [F + F_{,\phi\phi}] \tag{10b}$$

and

$$N_{\phi\theta} = -\frac{1}{R^2} \operatorname{cosec}\phi [F_{,\phi\theta} - \cot\phi F_{,\theta}] \tag{10c}$$

where  $F$  is a stress function and  $U = V = p_1 = p_2 = 0$ . Now substituting the inversions of equations (4a) to (4c) and equations (12a) to (12c) and (1d) to (1e) into the compatibility equation (3) gives

$$3(\nabla^2 + 2)u_{,\tau} + [2(\nabla^2 + 1) - 1](\nabla^2 + 2)\tilde{F} = 0 \tag{11a}$$

where

$$u = \frac{W'}{R}, \quad \tilde{F} = \frac{F\gamma^*}{khRC}, \quad C^2 = \frac{k}{\rho}, \quad \tau = \frac{C}{R}t \tag{11b-e}$$

and

$$\nabla^2(\cdot) = (\cdot)_{,\phi\phi} + \cot\phi(\cdot)_{,\phi} + \operatorname{cosec}^2\phi(\cdot)_{,\theta\theta}. \tag{11f}$$

The transverse equilibrium equations (9a) and (9b) can be written in the form

$$-u_{0,\tau\tau} + 2(1 + \alpha^2)\tilde{\sigma} + \tilde{P} = 0 \tag{12a}$$



and

$$u_{,\tau\tau} - \beta^2 (\nabla^2 + 2) \tilde{F} - \tilde{\sigma} \nabla^2 u + \alpha^2 \beta^2 [2(\nabla^2 + 1) + 1] (\nabla^2 + 2) u_{,\tau} = 0 \quad (12b)$$

respectively, when using equations (1), (4), (6)-(8) and (10)

and where

$$u_0 = \frac{\bar{W}}{R}, \quad \tilde{\sigma} = \frac{\bar{N}}{kh}, \quad \tilde{P} = \frac{P_3 R}{kh}, \quad \alpha^2 = \frac{1}{12} \left( \frac{h}{R} \right)^2$$

and

$$\beta^2 = \frac{C}{R\gamma^*}. \quad (12c-g)$$



### Chapter 3

#### Static Behavior

Equation (12a) predicts

$$\tilde{\sigma} = - \frac{\tilde{p}}{2} \quad (13)$$

when  $\alpha^2 \ll 1$ , while equations (11a) and (12b) become

$$\begin{aligned} [2(\lambda_n - 1) + 1](\lambda_n - 2)c_{mn} - \\ 3(\lambda_n - 2)a_{mn,\tau} = 0 \end{aligned} \quad (14a)$$

and

$$\begin{aligned} \beta^2(\lambda_n - 2)c_{mn} + \tilde{\sigma}\lambda_n a_{mn} + \\ \alpha^2\beta^2[2(\lambda_n - 1) - 1](\lambda_n - 2)a_{mn,\tau} = 0 \end{aligned} \quad (14b)$$

respectively, if it is assumed that

$$\begin{aligned} u = a_{on} P_n(\cos\phi) + \\ P_n^m(\cos\phi)(a_{mn} \cos m\theta + b_{mn} \sin m\theta) \end{aligned} \quad (15a)$$

and

$$\begin{aligned} \tilde{F} = c_{on} P_n(\cos\phi) + \\ P_n^m(\cos\phi)(c_{mn} \cos m\theta + d_{mn} \sin m\theta) \end{aligned} \quad (15b)$$

where

$$\lambda_n = n(n + 1) \quad (15c)$$

and  $P_n$  and  $P_n^m$  are Legendre and associated Legendre polynomials of degree  $n$  and order  $m$ . Two additional equations are also obtained but these are identical to equations (14a) and (14b) provide  $b_{mn}$  and  $d_{mn}$  are substituted for  $a_{mn}$  and  $c_{mn}$ . If  $c_{mn}$  is eliminated from equations (14a) and (14b), then





$$\beta^2 \tilde{\omega}_n a_{mn, \tau} + \tilde{\sigma} \lambda_n a_{mn} = 0 \quad (16a)$$

where

$$\tilde{\omega}_n = \frac{3(\lambda_n - 2)}{2\lambda_n - 1} + \alpha^2 (2\lambda_n - 3)(\lambda_n - 2). \quad (16b)$$

Now, substituting equation (13) into (16a) and integrating gives

$$a_{mn} = e^{\left( \frac{\tilde{P}}{2} \frac{\lambda_n}{\tilde{\omega}_n} \frac{1}{\beta^2} \frac{C}{R} t \right)} + K \quad (17)$$

where K is a constant of integration which is related to the initial imperfections in a shell.  $\beta^2$  which equals  $\frac{C}{R\gamma^*}$  depends on strain rate as  $\gamma^*$  depends on strain rate as shown in appendix B. With a strain rate near zero, as would be the case for static buckling  $\beta^2$  goes to infinity but  $1/\beta^2$  becomes

$$\frac{1}{\beta^2} = \frac{R\gamma^*}{C} = \frac{R}{C} \left( \frac{\dot{\epsilon}_e \gamma}{\dot{\epsilon}_e + \gamma} \right). \quad (18)$$

In the limit of  $\dot{\epsilon}_e$  very small,  $\dot{\epsilon}_e \ll \gamma$

$$\lim_{\dot{\epsilon}_e \rightarrow 0} \left( \frac{1}{\beta^2} \right) = \frac{R}{C} \dot{\epsilon}_e \quad (19)$$

where  $\dot{\epsilon}_e$  is the initial strain rate. Therefore equation (17) becomes

$$a_{mn} = e^{\left( \frac{\tilde{P}}{2} \frac{\lambda_n}{\tilde{\omega}_n} \dot{\epsilon}_e t \right)} + K \quad (20)$$

when  $\dot{\epsilon}_e \ll \gamma$ .

This equation is of the form of creep buckling.



## Chapter 4

### Dynamic Buckling

#### 4.1 Dominant Equation

From equation (12a)

$$u_o'_{\tau\tau} = 2\tilde{\sigma} \quad (21)$$

when  $\alpha^2 \ll 1$  and  $\tilde{P} = 0$ .  $\tilde{\sigma}$  is not time invariant and the solution of the above equation will be done in two parts.

The first part will assume the value of  $\tilde{\sigma}$  to be constant with time and the second will give the exact solution, then the two solutions will be equated at the final displacements. For buckling the dominant stress is defined as

$$\bar{N} = -h\sigma_e \quad (22)$$

and equation (21) becomes

$$u_o'_{\tau\tau} = -2\sqrt{3} \frac{\sigma_e}{\sigma_o} \quad (23)$$

The solution of equation (23) is

$$u_o = \frac{V_o}{C} \tau \left[ 1 - \frac{\tau}{2\tau_f} \right] \quad (24a)$$

when satisfying the initial conditions  $W = 0$  and  $\ddot{W} = V_o$  at  $t = 0$  and where

$$\tau_f = \frac{V_o}{2\sqrt{3}C} \left( \frac{\sigma_o}{\sigma_e} \right) \quad (24b)$$

is the time when  $\dot{W} = 0$ .



The exact solution uses equation (4a), (4b), (7a) and (7b) to revise  $\tilde{\sigma}$  to reflect the time dependence as follows

$$\bar{N} = \frac{kh}{\gamma^*} \quad 3 \left[ - \frac{\dot{\bar{W}}}{R} \right]. \quad (25)$$

Solving for  $\tilde{\sigma}$  and using equations (12c) and (2.9) yields

$$\tilde{\sigma} = \frac{\bar{N}}{kh} = - \frac{3}{2} - 3 \frac{C}{R\gamma} u_{O,\tau} \quad (26)$$

where

$$\dot{\epsilon}_e = 2 \frac{C}{R} u_{O,\tau}. \quad (27)$$

Substituting equation (26) into (21) produces

$$u_{O,\tau\tau} + \frac{6C}{R\gamma} u_{O,\tau} = -3 \quad (28)$$

the equation for the exact solution. The solution of equation (28) is

$$u_O = \frac{1}{12} \left( \frac{R\gamma}{C} \right)^2 \left( 1 + \frac{2V_O}{R\gamma} \right) \left[ 1 - e^{-\frac{6C}{R\gamma}\tau} \right] - \frac{R\gamma}{2C} \tau \quad (29a)$$

which satisfies the initial conditions  $W = 0$  and  $\dot{W} = V_O$  at  $t = 0$  and

$$\tau_f = \frac{R\gamma}{6C} \log_e \left( 1 + \frac{2V_O}{R\gamma} \right) \quad (29b)$$

is the time when  $\dot{W} = 0$ . Setting  $u_O(\tau_f)$  for the first solution equal to  $u_O(\tau_f)$  for the exact solution and solving for  $\sigma_O/\sigma_e$  one obtains

$$\frac{\sigma_O}{\sigma_e} = \frac{1}{\sqrt{3}} \left( \frac{R\gamma}{V_O} \right)^2 \left[ \frac{2V_O}{R\gamma} - \log_e \left( 1 + \frac{2V_O}{R\gamma} \right) \right] \quad (30)$$



therefore, the dominant solution may be taken as equation (24a) with (24b) and (30) used with it.

#### 4.2 Perturbation Equation

Using equations (15a-c) equation (12b) becomes

$$a_{mn,\tau\tau} - \beta^2(\lambda_n - 2)c_{mn} + \frac{\bar{N}}{kh} \lambda_n a_{mn} + \alpha^2 \beta^2 [2(\lambda_n - 1) - 1](\lambda_n - 2)a_{mn,\tau} = 0 \quad (31)$$

Solving equation (14a) for  $c_{mn}$  and substituting into equation (31) produces

$$a_{mn,\tau\tau} + \beta^2 \tilde{\omega}_n a_{mn,\tau} + \frac{\bar{N}}{kh} \lambda_n a_{mn} = 0 \quad (32a)$$

$$\text{where} \quad \lambda_n = n(n + 1) \quad (32b)$$

$$\tilde{\omega}_n = \frac{3(\lambda_n - 2)}{2\lambda_n - 1} + \alpha^2(2\lambda_n - 3)(\lambda_n - 2) \quad (32c)$$

$$\beta^2 = \frac{C}{R\gamma^*} = \left( \frac{1}{2u_{o,\tau}} + \frac{C}{R\gamma} \right). \quad (32d)$$

With a change of variable equation (32a) becomes

$$a_{mn,\xi\xi} - \tau_f \tilde{\omega}_n \left( \frac{C}{2V_o \xi} + \frac{C}{R\gamma} \right) a_{mn,\xi} - \tau_f^2 \left( \frac{3}{2} + \frac{3V_o}{R\gamma} \xi \right) \lambda_n a_{mn} = 0 \quad (33a)$$

$$\text{where} \quad \xi = 1 - \tau/\tau_f \quad (33b)$$





$$\frac{\bar{N}}{kh} = - \left[ \frac{3}{2} + \frac{3V_o}{R\gamma} \xi \right] \quad (33c)$$

and

$$u_o'_{,\tau} = \frac{V_o}{C} \xi. \quad (33d)$$

Putting equation (33a) into a format similar to Florence [8], one gets

$$a_{mn',\xi\xi} - \left[ Q_n^{(1)} + \frac{Q_n^{(2)}}{\xi} \right] a_{mn',\xi} - R_n^2 a_{mn} = 0 \quad (34a)$$

where

$$Q_n^{(1)} = \tau_f \frac{C}{R\gamma} \tilde{\omega}_n \quad (34b)$$

$$Q_n^{(2)} = \tau_f \frac{C}{2V_o} \tilde{\omega}_n \quad (34c)$$

and

$$R_n^2 = \tau_f^2 \left[ \frac{3}{2} + \frac{3V_o}{R\gamma} \xi \right] \lambda_n. \quad (34d)$$

As  $R_n^2$  is still a function of time ( $\xi$ ), in order to solve the equation using Florence's solution, the value of  $\left[ \frac{3}{2} + \frac{3V_o}{R\gamma} \xi \right]$  was set as a constant with respect to  $\xi$ . A value of 3/2 was used as we are primarily interested near  $\xi = 0$  which negates the influence of the second term, thus

$$R_n^2 \equiv 3/2 \tau_f^2 \lambda_n \quad (34e)$$

As given in Florence [8] the solution to equation (34a) is

$$a_{mn}(\xi) = A_{mn}(\xi) \alpha_n + B_{mn}(\xi) \beta_n \quad (35)$$



where

$$A_{mn}(\xi) = \frac{\Gamma(1 + a_n + b_n)}{\Gamma(2 + b_n)} \left[ \exp\{-(\Lambda_n + \Omega_n) + \Lambda_n \xi\} \right. \\
(\Omega_n \xi)^{1+b_n} \left[ - \{(\Lambda_n + 1 + b_n) U(\Omega_n) + \right. \\
\Omega_n U'(\Omega_n)\} M(\Omega_n \xi) + \{(\Lambda_n + 1 + b_n) M(\Omega_n) + \\
\left. \left. \Omega_n M'(\Omega_n)\} U(\Omega_n \xi) \right] \right] \quad (36a)$$

and

$$B_{mn}(\xi) = \frac{\Gamma(1 + a_n + b_n)}{\Gamma(2 + b_n)} \left[ \exp\{-(\Lambda_n + \Omega_n) + \right. \\
\left. \Lambda_n \xi\} \right] (\Omega_n \xi)^{1+b_n} \left[ U(\Omega_n) M(\Omega_n \xi) - \right. \\
\left. M(\Omega_n) U(\Omega_n \xi) \right] 2\tau_f \quad (36b)$$

In equations (36a) and (36b),  $M(\Omega_n \xi)$  and  $U(\Omega_n \xi)$  are shorthand notations to represent Kummer functions [15-17] (confluent hypergeometric functions) of the first and second kind, respectively, that is

$$M(\Omega_n \xi) \equiv M(1 + a_n + b_n, 2 + b_n, \Omega_n \xi) \quad (37a)$$

$$U(\Omega_n \xi) \equiv U(1 + a_n + b_n, 2 + b_n, \Omega_n \xi). \quad (37b)$$

Similarly

$$M(\Omega_n) \equiv M(1 + a_n + b_n, 2 + b_n, \Omega_n) \quad (37c)$$

$$U(\Omega_n) \equiv U(1 + a_n + b_n, 2 + b_n, \Omega_n) \quad (37d)$$



and primes over  $M(\Omega_n)$  and  $U(\Omega_n)$  denote differential coefficients with respect to  $\Omega_n \xi$  evaluated at  $\xi = 1$ . The remaining symbols are

$$a_n = \frac{\Omega_n^{(2)}}{2} \left[ \frac{\Omega_n^{(1)}}{\Omega_n} - 1 \right], \quad b_n = \Omega_n^{(2)} \quad (37e-f)$$

$$\Omega_n = \left( \Omega_n^{(1)^2} + 4R_n^2 \right)^{1/2}, \quad \Lambda_n = \frac{\Omega_n^{(1)} - \Omega_n}{2}. \quad (37g-h)$$



## Chapter 5

### Results and Discussion

Unfortunately, no experimental investigations appear to have been published on the dynamic instability of complete spherical shells and until recently no theoretical work had been published. The results reported herein will then be compared with previous experimental investigations into the behavior of impulsively loaded cylindrical shells and in theory with the publications now in press. Equation (5.2) from Appendix E predicts mode numbers which are  $3.173/3.624 = 0.876$  times as large as Jones and Ahn's [13] estimates for similar aluminum spherical shells and are  $3.173/74^{\frac{1}{2}} = 1.08$  times larger than Florence and Vaughan's [4] estimates for similar aluminum cylindrical shells. However, as shown in Figure 2, a plot of the first five sets of data from Table 1, the equation for the critical harmonic is

$$n = 2.0(R/h)^{.605} \quad (38)$$

which compares favorably with Lyons [6] curve with a slope of 0.625.

R/h	Critical Harmonic n
10	8
18.25	12
30	15
50	21
100	32

Table 1: A Comparison of the Critical Mode Numbers for a Visco-plastic Spherical Shell with Differing R/h values, with  $R = 1.460$  in.,  $V_0 = 9357.6$  in/sec,  $\gamma = 6500 \text{ sec}^{-1}$ ,  $\sigma_0 = 46,000$  psi and  $\rho = 0.0002523 \text{ lb-sec}^2/\text{in.}^4$ .





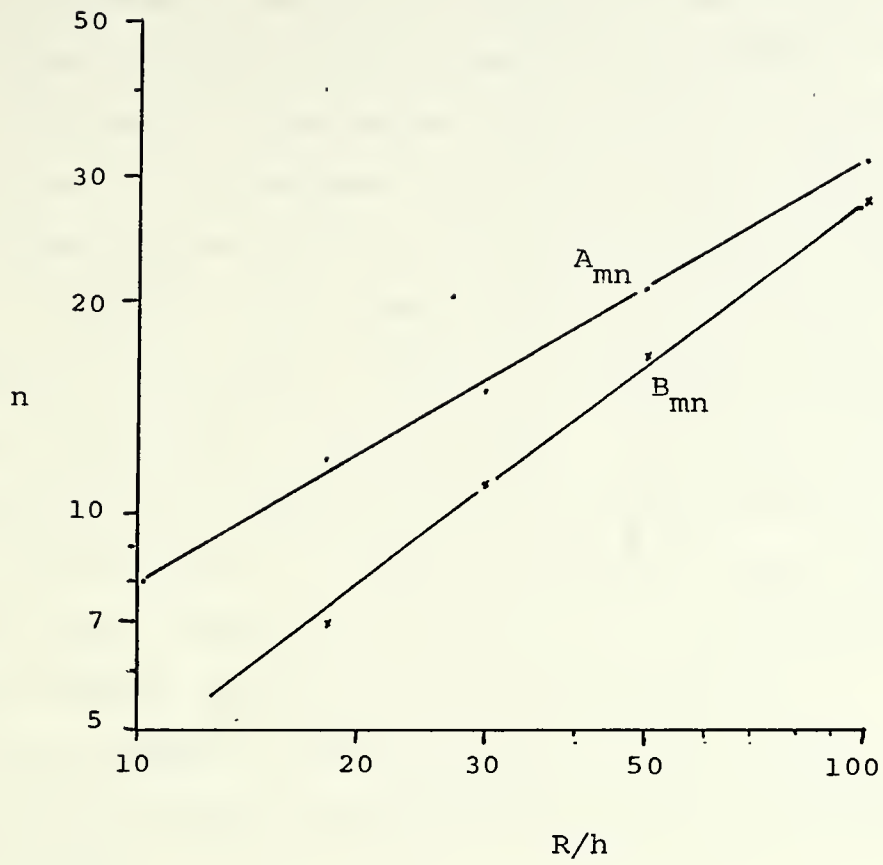


Figure 2: Critical Mode of Buckling as a Function of  $R/h$  with  $V_0 = 9357.58$  in/sec and  $\gamma = 6500 \text{ sec}^{-1}$ .



Figure 3 shows the growth of the amplitude function with regard to time for the continuous spectrum of the mode numbers  $n$ . Showing addition figures later, this growth is faster for larger  $V_0$ , larger  $\gamma$  and for later stages of the process (small  $\xi$ ). The change of preferred buckling mode is shown by a dashed line. It is evident from Table 2a that equation (38) provides a reasonable estimate of the preferred mode of the amplification function which is obtained numerically from the corresponding theoretical analysis using Kummer's functions and numerical integration of the equations. The use of the Kummer's functions for solution ran into problems because of the size of the functions and that differences of these very large numbers were removing the first five or six significant figures. Even double precision was not eliminating the problem, for the asymptotic expansion [16] is a truncating series and even with double precision can't give the necessary significant figures.

The Florence method gave good results that correlated well, up to four significant figures, with the numerical method. The problem with the Florence method occurred when the values of inputs to the Kummer function became so large i.e. greater than 8 that one has to use an asymptotic expansion. Also the last couple of computations with values just less than 8 one loses some accuracy. As was observed by Florence [8] and Wojewodzki [11] the critical modes of viscoplastic cylinders were constantly lower than modes of rigid-plastic cylinders. Likewise as shown from Table 2a,



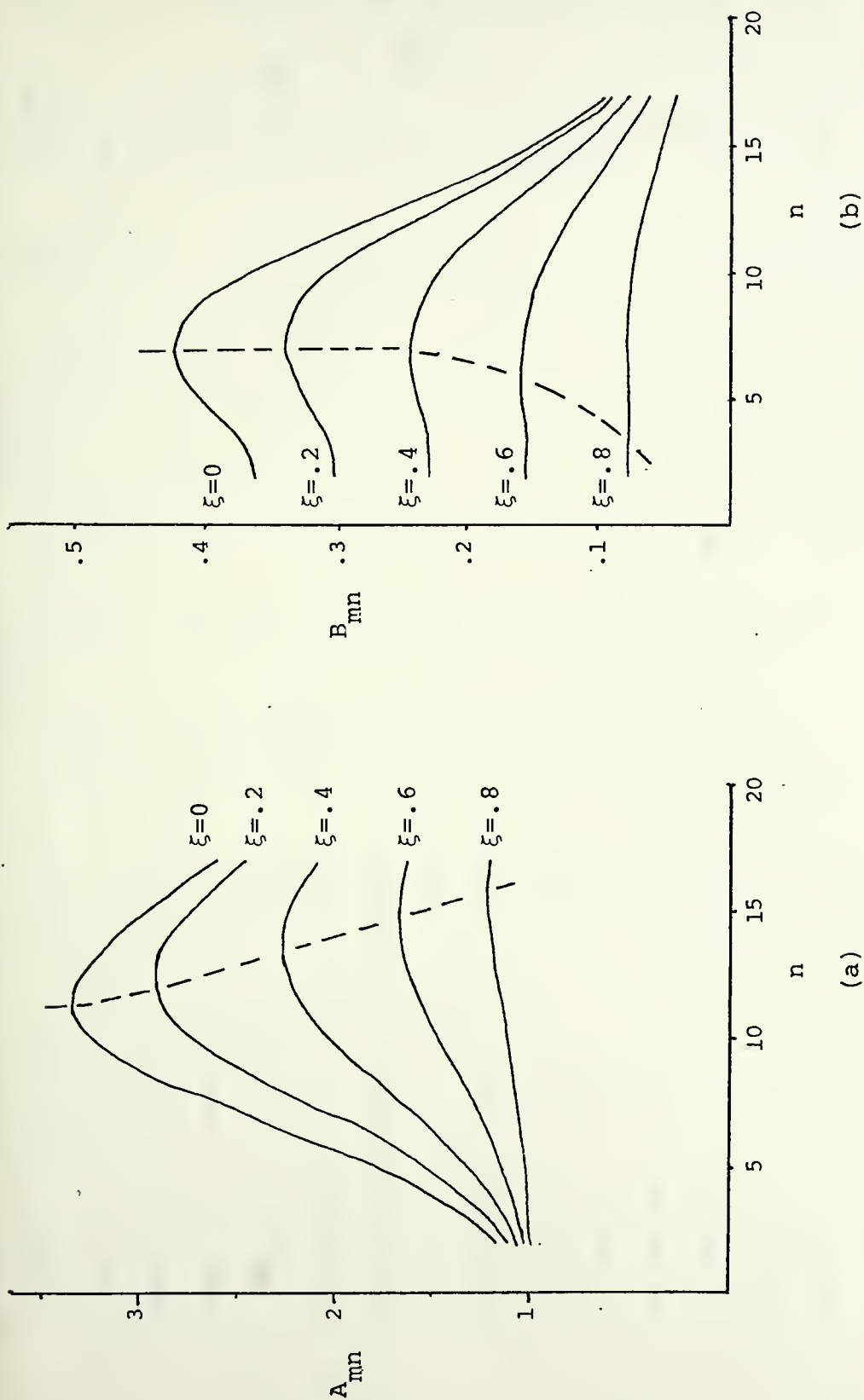


Figure 3: Amplification Function at  $\tau = .2, .4, .6, .8$  and  $1.0 \tau_f$  for (a) Displacement and (b) Velocity Imperfections for a Viscoplastic Spherical Shell with  $R = 1.460$  in.,  $R/h = 18.25$ , and  $\gamma = 6500 \text{ sec}^{-1}$ .



Material	R(in)	R/h	V <sub>o</sub> (in/sec)	Florence's Method			Numerical Integration		EQ. (38)	Expt. Cylinder	Ref.
				A <sub>mn</sub> (0)	B <sub>mn</sub> (0)	A <sub>mn</sub> (0)	B <sub>mn</sub> (0)	A <sub>mn</sub> (0)			
1.	Steel 1015	1.494	10.4	5040.0	8	-	8	-	-	11	[1]
2.	Steel 1015	1.495	16.8	6000.0	11	5	10	-	-	15	[1]
3.	Steel 1015	1.494	22.6	5880.0	12	6	12	5	-	16	[1]
4.	Steel 1015	1.493	35.6	4560.0	16	8	15	6	-	28	[1]
5.	AL 2024 T3	1.495	9.9	8040.0	8	4	8	-	-	12	[1]
6.	AL 2024 T3	1.495	15.0	7080.0	10	5	10	4	-	12	[1]
7.	AL 2024 T3	1.495	19.4	9360.0	12	8	12	7	-	16	[1]
8.	AL 6061 T6	1.487	9.9	6480.0	8	-	8	-	8	9	[1]
9.	AL 6061 T6	1.488	14.7	6840.0	10	6	10	5	10	15	[1]
10.	AL 6061 T6	1.488	14.7	7440.0	10	6	10	5	10	16	[1]
11.	AL 6061 T6	1.490	19.6	7800.0	12	8	12	7	12	18	[1]
12.	AL 6061 T6	1.490	19.6	7680.0	12	8	12	7	12	18	[1]
13.	AL 6061 T6	1.453	15.3	4175.8	10	-	10	-	10	11-16	[5]
14.	AL 6061 T6	1.459	17.6	4571.7	11	5	11	-	11	14-15	[5]

Table 2a: A Comparison of the Critical Mode Numbers for a Viscoplastic Spherical Shell with the Corresponding Experimental Results on Cylindrical Shells. (Continued)





	Material	R(in)	R/h	$V_o$ (in/sec)	Florence's Method		Numerical Integration		EQ. (38)	Expt. Cylinder	Ref.
					$A_{mn}(0)$	$B_{mn}(0)$	$A_{mn}(0)$	$B_{mn}(0)$			
15.	AL 6061 T6	1.468	22.6	5572.4	13	7	12	6	13	19-20	[5]
16.	AL 6061 T6	1.468	22.6	5749.3	13	8	12	6	13	15-16	[5]
17.	AL 6061 T6	1.495	9.9	6469.0	8	-	8	-	8	9	[6]
18.	AL 6061 T6	1.485	14.7	6993.4	10	6	10	5	10	15	[6]
19.	AL 6061 T6	1.485	14.7	7505.1	10	6	10	5	10	16	[6]
20.	AL 6061 T6	1.460	18.25	4678.8	11	5	11	-	12	-	[6]
21.	AL 6061 T6	1.460	18.25	5398.6	11	6	11	4	12	-	[6]
22.	AL 6061 T6	1.460	18.25	5758.5	11	6	11	5	12	14	[6]
23.	AL 6061 T6	1.460	18.25	9357.6	12	7	12	7	12	15	[6]
24.	AL 6061 T6	1.490	19.6	8252.5	12	8	12	7	12	18	[6]
25.	AL 6061 T6	1.490	19.6	7798.2	12	8	12	7	12	18	[6]
26.	AL 6061 T6	1.464	20.92	8127.0	13	9	12	8	13	20-21	[6]
27.	AL 6061 T6	1.475	29.5	5522.7	15	9	14	8	15	23	[6]
28.	AL 6061 T6	1.475	29.5	7133.5	15	11	15	9	15	25	[6]

Table 2a: A Comparison of the Critical Mode Numbers for a Viscoplastic Spherical Shell with the Corresponding Experimental Results on Cylindrical Shells. (Continued)



Material	R(in)	R/h	V <sub>O</sub> (in/sec)	Florence's		Numerical		EQ. (38)	Expt. Cylinder	Ref.
				Method		Integration				
				A <sub>mn</sub> (0)	B <sub>mn</sub> (0)	A <sub>mn</sub> (0)	B <sub>mn</sub> (0)			
29. AL 6061 T6	1.475	29.5	9204.6	15	11	15	11	15	24	[6]
30. Steel 1015	1.510	10.5	2089.0	8	-	8	-	-	9	[7]
31. Steel 1015	1.510	10.5	2411.0	8	-	8	-	-	9	[7]
32. Steel 1015	1.510	10.5	2893.0	8	-	8	-	-	9	[7]
33. Steel 1015	1.510	10.5	4581.0	8	-	8	-	-	9	[7]
34. Steel 1015	1.488	16.7	3251.0	10	-	10	-	-	14	[7]
35. Steel 1015	1.488	16.7	3381.0	10	-	10	-	-	14	[7]
36. Steel 1015	1.488	16.7	4551.0	11	5	11	5	-	13	[7]
37. Steel 1015	1.502	22.8	1921.0	12	-	12	-	-	22	[7]
38. Steel 1015	1.502	22.8	2241.0	12	-	12	-	-	19-22	[7]
39. Steel 1015	1.502	22.8	4162.0	13	7	13	7	-	19	[7]
40. Steel 1015	1.494	35.6	2875.0	16	8	16	8	-	26	[7]
41. Steel 1051	1.494	35.6	3354.0	16	9	16	9	-	26	[7]

Table 2a: A Comparison of the Critical Mode Numbers for a Viscoplastic Spherical Shell with the Corresponding Experimental Results on Cylindrical Shells.



Material	Ref.	$\sigma_0$ (ksi)	$\rho$ (lb-sec <sup>2</sup> /in. <sup>4</sup> )	$\gamma$ sec <sup>-1</sup>
Steel 1015	[1]	102	.0007324	40.4
AL 2024 T3	[1]	56	.0002523	6500
AL 6061 T6	[1]	44	.0002523	6500
AL 6061 T6	[5]	44	.0002525	6500
AL 6061 T6	[6]	46	.0002523	6500
Steel 1015	[7]	30	.0007324	40.4

Table 2b: Values of  $\sigma_0$ ,  $\rho$  and  $\gamma$  that Correspond to Materials in Table 2a.



Material No.	$\tau_f$ EQ. (24b)	C (10 <sup>3</sup> in/sec) EQ. (11d)
1	.094	16.1
2	.110	16.3
3	.108	16.3
4	.085	16.0
5	.158	15.4
6	.140	15.3
7	.182	15.5
8	.146	13.5
9	.153	13.5
10	.166	13.6
11	.173	13.6
12	.171	13.6
13	.097	13.2
14	.105	13.2
15	.127	13.4
16	.130	13.4
17	.142	13.8
18	.153	13.8
19	.164	13.9
20	.105	13.6

Table 2c: Values of  $\tau_f$  and C that Correspond to Materials  
in Table 2a. (Continued)





Material No.	$\tau_f$ EQ. (24b)	$C(10^3 \text{ in/sec})$ EQ. (11d)
21	.120	13.7
22	.128	13.7
23	.200	14.1
24	.179	14.0
25	.169	13.9
26	.179	14.0
27	.123	13.7
28	.156	13.9
29	.198	14.1
30	.118	8.5
31	.103	8.4
32	.145	8.6
33	.082	8.3
34	.071	8.2
35	.157	8.7
36	.119	8.5
37	.115	8.5
38	.158	8.7
39	.103	8.4
40	.087	8.3
41	.076	8.2

Table 2c: Values of  $\tau_f$  and C that Correspond to Materials  
in Table 2a.



the critical modes of spherical shells are considerably lower than those observed experimentally on cylindrical shells with the same material parameters and  $R/h$  ratios which were tested by the authors of references [1, 5, 6, 7], with the further observation that correlation seems to be closer at lower  $R/h$  values. Of course,  $n$ , in the present case, refers to the critical or most amplified harmonic\* in the displacement field of a complete spherical shell which is expressed in terms of Legendre and associated Legendre polynomials (equation (15a)), while in reference [4] on cylindrical shells, it is associated with trigonometric functions.

The concept of threshold or critical impulse has been used by numerous investigators to mark the smallest impulse that a structure can tolerate without excessive deformation. It is evident from Figure 4 which is a plot of Table 3 that the displacement amplification function is a highly non-linear function of the impulsive velocity ( $V_0$ ). The critical velocity is very dependent on the value of  $\gamma$  used as shown in Figure 4.

It is evident from Figure 4 that the displacement functions at  $\tau = \tau_f$  experience larger amplifications than do the velocity functions. As stated by Jones and Ahn [13], this suggests that shape imperfections might exercise a much more significant influence on the instability of spherical shells than variations in the initial velocity field.

---

\*The critical harmonics are always rounded off to the nearest integer.



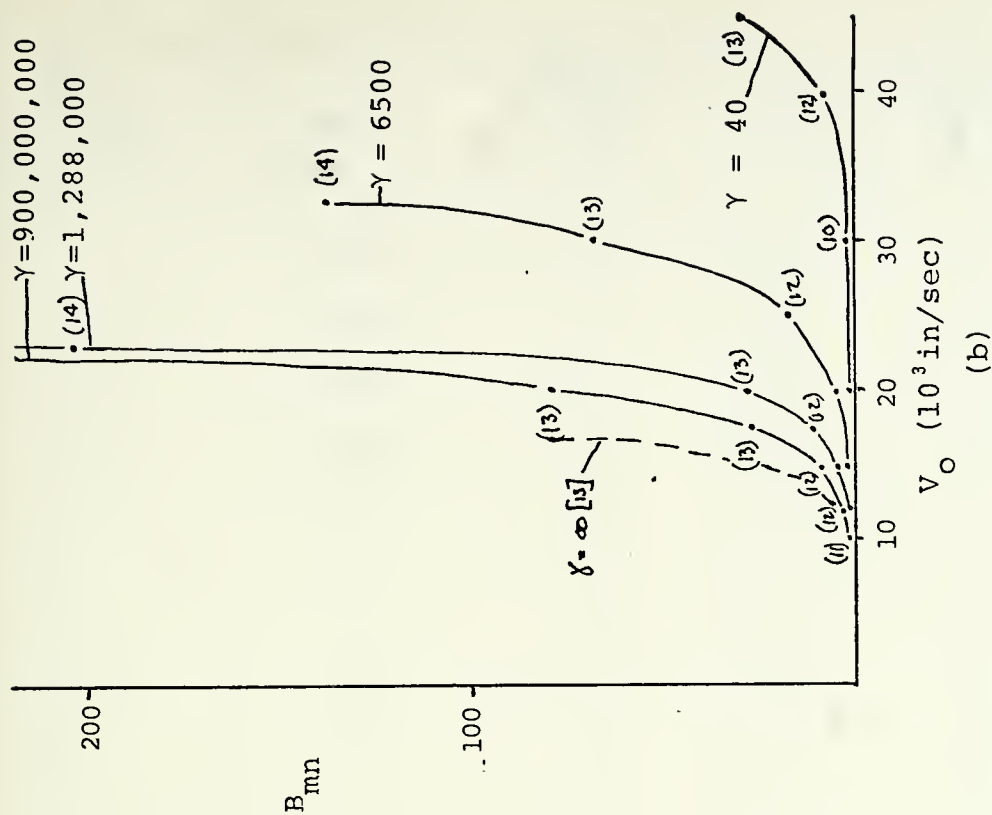
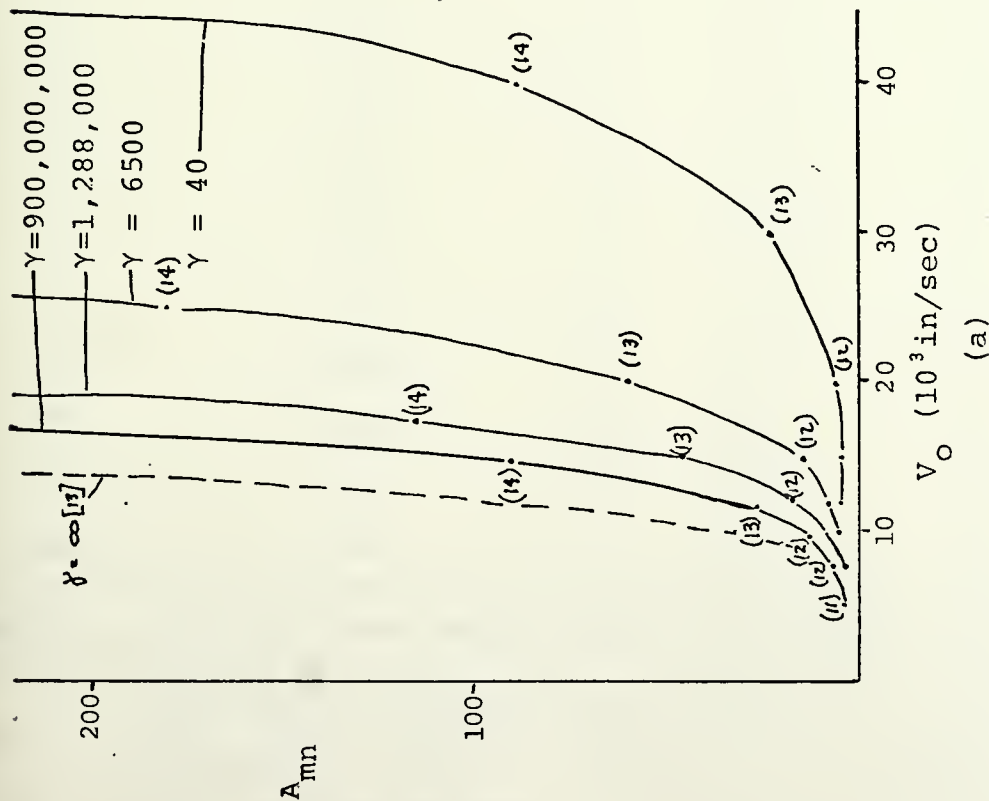


Figure 4: Variation of Largest Amplification Functions at  $\tau = \tau_f$  with Initial Impulsive Velocity for (a) Displacement and (b) Velocity Imperfections for a Viscoplastic Spherical Shell with  $R = 1.460$  in.,  $P/h = 18.25$  and Various Values of  $\gamma$ . The Numbers in Parentheses ( ) are the Critical Modes for  $A_{mn}(0)$  and  $B_{mn}(0)$ .



$V_0$ (10 in/sec)	$\gamma$ $\text{sec}^{-1}$	Critical Mode n	$A_{mn}$	Critical Mode n	$B_{mn}$
5	40	11	1.21	2	0.12
7.5	40	11	1.47	2	0.18
10	40	11	1.85	5	0.24
11	40	11	2.05	5	0.26
12	40	11	2.28	6	0.29
15	40	11	3.17	7	0.40
20	40	12	5.81	8	0.70
30	40	13	21.6	10	2.38
40	40	14	88.6	12	9.07
45	40	14	332.	13	28.6
5	6500	11	1.60	2	0.19
7.5	6500	11	2.51	6	0.31
10	6500	12	4.22	8	0.50
11	6500	12	5.28	8	0.61
12	6500	12	6.64	9	0.75
15	6500	12	13.6	10	1.45
20	6500	13	48.8	11	4.81
25	6500	14	190.	12	17.4
30	6500	15	788.	13	68.4
32.5	6500	15	1644.	14	138.

Table 3: Critical Mode Numbers and Displacement Function  
Amplitudes Versus Initial Velocities at Differing  
Values of  $\gamma$  with  $R = 1.460$  in.,  $R/h = 18.25$ ,  
 $\sigma_0 = 46,000$  psi and  $\rho = 0.0002523$  lb-sec<sup>2</sup>/in.<sup>4</sup>. (Cont.)





$V_o$ (10 in/sec)	$\gamma$ $\text{sec}^{-1}$	Critical Mode n	$A_{mn}$	Critical Mode n	$B_{mn}$
5	1,288,000	11	1.99	5	0.25
7.5	1,288,000	12	3.85	8	0.48
10	1,288,000	12	8.26	9	0.96
11	1,288,000	12	11.4	10	1.28
12	1,288,000	13	15.9	10	1.76
15	1,288,000	13	45.7	11	4.73
17.5	1,288,000	14	116.	12	11.4
20	1,288,000	14	304.	13	28.6
25	1,288,000	15	2334.	14	205.
5	900,000,000	11	2.24	6	0.29
7.5	900,000,000	12	4.89	8	0.61
10	900,000,000	12	11.7	10	1.35
11	900,000,000	13	17.5	10	1.98
12	900,000,000	13	25.7	11	2.81
15	900,000,000	14	89.4	12	9.19
17.5	900,000,000	14	274.	13	26.6
20	900,000,000	15	856.	13	80.3
22.5	900,000,000	15	2902.	14	252.

Table 3: Critical Mode Numbers and Displacement Function  
Amplitudes Versus Initial Velocities at Differing  
Values of  $\gamma$  with  $R = 1.460$  in.,  $R/h = 18.25$ ,  
 $\sigma_o = 46,000$  psi and  $\mu = 0.0002523$  lb-sec<sup>2</sup>/in.<sup>4</sup>.



It should be noted that the present theory is an approximate one since the linearized form of the constitutive equations for rate-sensitive material were used. In addition to the various simplifications and approximations which were introduced in the theoretical analysis, the influence of transverse shear stresses and deformations have been disregarded. Also, the influence of unloading has been neglected so that the effect of possible plastic behavior after  $\tau = \tau_f$  has not been considered. Moreover, the influence of wave disturbance has been neglected. However, with final times ( $t_f$ ) being in the neighborhood of 10-30  $\mu\text{sec}$ , which can be calculated by using equation (11e) and Table 2c, then one should not neglect wave phenomena. As an example materials 1, 10, 20, 30, 40 have values of  $t_f = 8.7, 13.2, 11.3, 29.1,$  and  $15.9 \mu\text{sec}$ , respectively.



## Chapter 6

### Conclusions

A theoretical investigation has been undertaken into the dynamic instability of complete spherical shells which are made from a viscoplastic material and loaded impulsively. Unfortunately, no experimental results are available to examine the validity, or otherwise, of the various theoretical predictions. However, the forms of the expressions for the critical mode number and threshold velocity are similar to those developed for cylindrical shells and spherical shells, except that the magnitude of the numerical coefficients are different. The threshold velocities for viscoplastic spherical shells came out higher than that for rigid plastic spherical shells with the same  $R/h$  ratios and material parameters. The viscoplastic theory predicts critical mode numbers for spherical shells which are similar to those observed experimentally on cylindrical shells with  $10 < R/h < 30$  but the correlation was better at the lower range the critical mode numbers were only one to three less than the rigid-plastic prediction where as the higher range produced mode numbers of four to eight less than the rigid plastic prediction.



## Chapter 7

### Recommendations

To further the investigation of viscoplastic effects, the next logical step would be to look into the non-linear constitutive equations. This may result in a sufficient enough change so as to correct some of the problems of the threshold velocities.





## References

1. J. N. Goodier & G. R. Abrahamson, "Dynamic Plastic Flow Buckling of a Cylindrical Shell from Uniform Radial Impulse", Proc. 4th U.S. Nat. Cong. App. Mechs., ASME, Berkely, Calif., 1962.
2. J. N. Goodier, "Dynamic Plastic Buckling", Proc. 1 Mat. Conf. on "Dynamic Stability of Structures", Northwestern University, Illinois, Oct. 1965, Edited G. Herrimann, pub. Pergamon Press, 1967.
3. A. L. Florence & J. N. Goodier, "Dynamic Plastic Buckling of Cylindrical Shells in Sustained Axial Compression Flow", Trans. of ASME, Journal of Applied Mechanics, Vol. 35, pp 80-86, March 1968.
4. A. L. Florence & H. Vaughan, "Dynamic Plastic Flow Buckling of Short Cylindrical Shells Due to Impulsive Loading", Int. Journal Solids Structures, Vol. 4, pp 741-756, Pergamon Press, 1968.
5. H. Vanghan & A. L. Florence, "Plastic Flow Buckling of Cylindrical Shells Due to Impulsive Loading", Journal of Applied Mechanics, Vol. 37, pp 171-179, 1970.
6. W. C. Lyons, "Elastic and Plastic Buckling of Cylindrical Shells Subjected to Impulsive Loads", Archivum Mechaniki Strosowanej, 1, 22, pp 111-124, 1970.
7. A. L. Florence, "Buckling of Viscoplastic Cylindrical Shells Due to Impulsive Loading", AIAA Journal, Vol. 6, No. 3, March 1968.
8. A. L. Florence, "Dynamic Buckling of Viscoplastic Cylindrical Shells", 4th Mat. Science Colloquia on "Inelastic Behavior of Solids", Battelle Institute, Ohio, Sept. 1969, McGraw Hill, 1970.
9. W. Wojewodzki, "Dynamic Buckling a Viscoplastic Cylindrical Shell Subjected to Axial Impact", Archives for Mechanics, 23, 1, pp 73-91, Warszawa, 1971.
10. W. Wojewodzki, "Buckling of Viscoplastic Cylindrical Shells Loaded by Radial Pressure Impulse", Archives of Mechanics, 24, 5-6, pp 777-792, Warszawa, 1972.
11. W. Wojewodzki, "Buckling of Short Viscoplastic Cylindrical Shells Subjected to Radial Impulse", Int. Journal Non-Linear Mech., Vol. 8, pp 325-343, Pergamon Press, 1973.



12. N. Jones & C. S. Ahn, "Dynamic Plastic Buckling of Complete Spherical Shells", MIT, Dept. of Ocean Eng., Report No. 73-19, 1973.
13. N. Jones & C. S. Ahn, "Dynamic Buckling of Complete Rigid-Plastic Spherical Shells", Journal of Applied Mechanics, in press.
14. N. Jones & C. S. Ahn, "Dynamic Elastic and Plastic Buckling of Complete Spherical Shells", International Journal of Solids and Structures, in press.
15. "Handbook of Mathematical Functions", Edited by M. Abramowitz and I. A. Stegun, pp 504-514, Dover Publications, Inc., New York.
16. A. D. MacDonald, "Properties of the Confluent Hypergeometric Function", Technical Report 84, Research Laboratory of Electronics, MIT, November 18, 1948.
17. E. T. Whittaker & G. N. Watson, "A Course of Modern Analysis", Cambridge University Press, England, 1963.
18. P. Perzyna, "The Constitutive Equations for Rate Sensitive Plastic Materials", Quarterly of Applied Mathematics, Vol. 20, No. 4, pp 321-322, January 1963.
19. S. R. Bodner & P. S. Symonds, "Experimental and Theoretical Investigations of the Plastic Deformation of Cantilever Beams Subjected to Impulsive Loading", Journal of Applied Mechanics, Vol. 29, pp 719-728, 1962.
20. M. J. Manjone, "Influence of Rate of Strain and Temperature on Yield Stresses in Mild Steel", Journal Applied Mechanics, Vol. 11, pp 211, 1944.
21. E. W. Parks, "The Permanent Deformation of a Cantilever Struck Transversely at its Tip", Proc. A. Soc., Vol. 228, 1955.



## Appendix A

### Constitutive Equations of Viscoplastic Spherical Shells

The constitutive equations for cylindrical shells which are made from a rigid viscoplastic material are developed in references [8], [10], [11], and [18]. This appendix contains a brief derivation of constitutive equations for viscoplastic spherical shells.

Consider a special linearized case of the constitutive equations for a rate-sensitive plastic material as derived by Perzyna [18]

$$\dot{\epsilon}_{ij} = 2k\gamma F \frac{\partial F}{\partial \sigma_{ij}} \quad (1.1)$$

where  $\dot{\epsilon}_{ij}$  and  $\sigma_{ij}$  are components of the plastic strain rate and stress tensors,  $k$  is the yield stress in simple shear and  $\gamma$  is a physical constant of the material later termed the viscosity constant.  $\gamma$  is obtained by uniaxial tests as described later. In the above equation the function  $F$ , a function of strain rate and stress, is defined by  $F = \sqrt{J_2}/k - 1$  where  $J_2 = 1/2 S_{ij} S_{ij}$  is the second invariant of the stress deviator with components  $S_{ij}$ . In accordance with the Levy-Mises flow rule for rigid perfectly plastic material, as  $\gamma \rightarrow \infty$ ,  $J_2 = k^2$  where  $k = \sigma_0/\sqrt{3}$ .

The results of uniaxial stress experiments produced the Cowper and Symonds [19] power-type relation

$$\sigma_e = \sigma_0 \left[ 1 + \left( \frac{\dot{\epsilon}_e}{\gamma} \right)^{1/\delta} \right] \quad (1.2)$$



which give the non-linearized form of function F. Inverting (1.2) we get

$$\dot{\epsilon}_e = \gamma \left( \frac{\sigma_e}{\sigma_0} - 1 \right)^\delta \quad (1.3a)$$

where  $\sigma_e$  and  $\dot{\epsilon}_e$  are the equivalent stress  $[\frac{3}{2} S_{ij} S_{ij}]^{\frac{1}{2}}$  and strain rate  $[\frac{2}{3} \dot{\epsilon}_{ij} \dot{\epsilon}_{ij}]^{\frac{1}{2}}$  respectively and  $\sigma_0$  is the static uniaxial yield stress of the material and  $\gamma$  and  $\delta$  are constants obtained experimentally for a given material

$$\sigma_e = [\sigma_{11}^2 + \sigma_{11} \sigma_{22} + \sigma_{22}^2 + 3\sigma_{12}^2]^{\frac{1}{2}} \quad (1.3b)$$

$$\dot{\epsilon}_e = \frac{2}{\sqrt{3}} [\dot{\epsilon}_{11}^2 + \dot{\epsilon}_{11} \dot{\epsilon}_{22} + \dot{\epsilon}_{22}^2 + 3\dot{\epsilon}_{12}^2]^{\frac{1}{2}}. \quad (1.3c)$$

Taking the linearized form of equation (1.2) we get

$$\sigma_e = \sigma_0 \left( 1 + \frac{\dot{\epsilon}_e}{\gamma} \right) \quad (1.4)$$

where  $\gamma$  is redefine as explained in Appendix B.

In the case of plane stress ( $\sigma_{13} = \sigma_{23} = \sigma_{33} = 0$ ) equation (1.1) yields the following equations.

$$\dot{\epsilon}_{11} = \frac{\gamma}{3} \left( \frac{\sqrt{J_2}}{k} - 1 \right) \frac{2\sigma_{11} - \sigma_{22}}{\sqrt{J_2}} \quad (1.5a)$$

$$\dot{\epsilon}_{22} = \frac{\gamma}{3} \left( \frac{\sqrt{J_2}}{k} - 1 \right) \frac{2\sigma_{22} - \sigma_{11}}{\sqrt{J_2}} \quad (1.5b)$$

$$\dot{\epsilon}_{12} + \dot{\epsilon}_{21} = 2\gamma \left( \frac{\sqrt{J_2}}{k} - 1 \right) \frac{\sigma_{12}}{\sqrt{J_2}} \quad (1.5c)$$





where  $J_2 = \frac{1}{3} \sigma_e^2$ ,  $k = \sigma_o / \sqrt{3}$ . (1.5d-e)

Inverting equations (1.5a-c) produces.

$$\sigma_{11} = \frac{k}{\gamma^*} (2\dot{\epsilon}_{11} + \dot{\epsilon}_{22}) \quad (1.6a)$$

$$\sigma_{22} = \frac{k}{\gamma^*} (2\dot{\epsilon}_{22} + \dot{\epsilon}_{11}) \quad (1.6b)$$

$$\sigma_{12} = \frac{k}{\gamma^*} \left( \frac{\dot{\epsilon}_{12} + \dot{\epsilon}_{21}}{2} \right). \quad (1.6c)$$

where  $\gamma^* = \gamma(1 - k/\sqrt{J_2}) = \gamma(1 - \sigma_o/\sigma_e)$ . (1.6d)

Now, assume that the strain rates can be represented as follows:

$$\dot{\epsilon}_{11} = \dot{\epsilon}_1 + z \dot{\kappa}_1 \quad (1.7a)$$

$$\dot{\epsilon}_{22} = \dot{\epsilon}_2 + z \dot{\kappa}_2 \quad (1.7b)$$

$$\dot{\epsilon}_{12} + \dot{\epsilon}_{21} = \dot{\epsilon}_{12} + z \dot{\kappa}_{12}. \quad (1.7c)$$

Considering that  $\gamma^*$  is not constant and in fact is a function of  $z$ , one assumes that the variation of  $\gamma^*$  with  $z$  is second order, a perturbation quantity. As shown in appendix B  $\gamma^*$  is dependent on  $\dot{\epsilon}_e$  and as shown in Figure 5,  $\dot{\epsilon}_1 = \dot{\bar{\epsilon}}_1 + \dot{\epsilon}'_1$  where  $\dot{\epsilon}'_1$  is a perturbation quantity dependent on  $z$ . Therefore,  $\gamma^*$  can be taken as a function of  $\dot{\bar{\epsilon}}_e$  and not a function of  $z$ . Now the constitutive equations can be integrated out as

$$N_1 = \int_{-h/2}^{h/2} \sigma_1 dz = \frac{kh}{\gamma^*} (2\dot{\epsilon}_1 + \dot{\epsilon}_2) \quad (1.8a)$$



$$N_2 = \int_{-h/2}^{h/2} \sigma_2 dz = \frac{kh}{\gamma^*} (2\dot{e}_2 + \dot{e}_1) \quad (1.8b)$$

$$N_{12} = \int_{-h/2}^{h/2} \sigma_{12} dz = \frac{kh}{\gamma^*} \frac{\dot{e}_{12}}{2} \quad (1.8c)$$

$$M_1 = \int_{-h/2}^{h/2} \sigma_1 z dz = \frac{kh^3}{12\gamma^*} (2\dot{\kappa}_1 + \dot{\kappa}_2) \quad (1.8d)$$

$$M_2 = \int_{-h/2}^{h/2} \sigma_2 z dz = \frac{kh^3}{12\gamma^*} (2\dot{\kappa}_2 + \dot{\kappa}_1) \quad (1.8e)$$

$$M_{12} = \int_{-h/2}^{h/2} \sigma_{12} z dz = \frac{kh^3}{12\gamma^*} \frac{\dot{\kappa}_{12}}{2} \quad (1.8f)$$



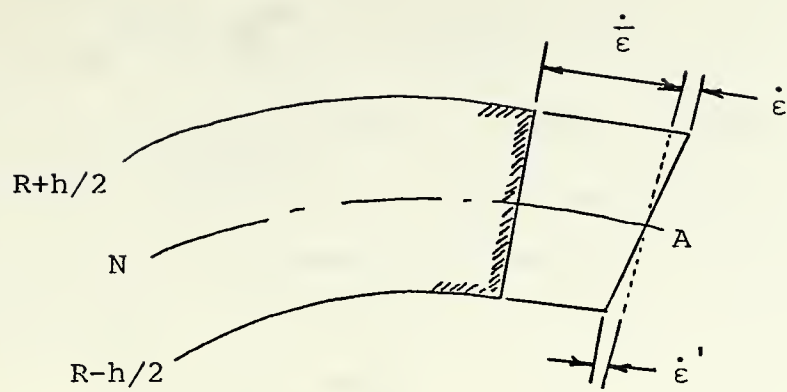


Figure 5: Variation of Strain Rate Across Thickness of Section.



## Appendix B

### Variations of $\gamma$ and $\sigma_o$

Equation (1.4) from Appendix A is shown in figure 6 along with a straight line tangent to the Cowper and Symonds power type relation as suggested by Florence [7]. The equation Florence suggested is

$$\sigma_e = \sigma_{01} + \mu \dot{\epsilon}_e \quad (2.1)$$

where  $\mu$  is the slope of the tangent line, tangent at the maximum initial strain rate  $\dot{\epsilon}_e^*$ , and  $\sigma_{01}$  is the intercept of this tangent line at static test strain rate. The slope of the tangent line is obtained by differentiations of equation (1.2) and evaluating the results at  $\dot{\epsilon}_e^*$

$$\left. \frac{d\sigma_e}{d\dot{\epsilon}_e} \right|_{\dot{\epsilon}_e = \dot{\epsilon}_e^*} = \mu = \frac{\sigma_o}{\delta \gamma^{1/\delta} \dot{\epsilon}_e^{*1-1/\delta}} \quad (2.2)$$

The value of  $\sigma_{01}$  is now obtained by equation equation (2.1) and (1.2) evaluated at  $\dot{\epsilon}_e^*$

$$\sigma_{01} = \sigma_o \left[ 1 + \left( \frac{\dot{\epsilon}_e^*}{\gamma} \right)^{1/\delta} \left( 1 - \frac{1}{\delta} \right) \right] \quad (2.3)$$

Putting equation (2.1) into the form of equation (1.4)

$$\sigma_e = \sigma_{01} \left( 1 + \frac{\dot{\epsilon}_e}{\sigma_{01}^{\mu}} \right) \quad (2.4)$$





where now  $\sigma_{01}$  and  $\sigma_{01}/\mu$  compare with  $\sigma_o$  and  $\gamma$  from equation (1.4), respectively. Letting  $\sigma_{01}/\mu = \gamma_1$

$$\gamma_1 = \delta \dot{\epsilon}_e^* \left[ \left( \frac{\gamma}{\dot{\epsilon}_e^*} \right)^{1/\delta} + \left( 1 - \frac{1}{\delta} \right) \right] \quad (2.5)$$

and

$$\sigma_e = \sigma_{01} \left( 1 + \frac{\dot{\epsilon}_e}{\gamma_1} \right). \quad (2.6)$$

A replacement of  $\sigma_o$  and  $\gamma$  with  $\sigma_{01}$  and  $\gamma_1$  respectively in the equations would give the identical solution with the result being the use of the tangent line approximation.

The values of the material constants are  $\delta = 5$  and  $\gamma = 40.4 \text{ sec}^{-1}$  for hot rolled mild steel [20] and  $\delta = 4$  and  $\gamma = 6500 \text{ sec}^{-1}$  for 6061 T6 aluminum [21]. For thin spherical shells of radius  $R$  the initial strain rate is computed as  $\dot{\epsilon}_e^* = 2V_o/R$ , where  $V_o$  is the uniform initial velocity.

From Chapter 2 equation (5b)

$$\gamma^* = \gamma(1 - \sigma_o/\sigma_e) \quad (2.7a)$$

where  $k = \sigma_o/\sqrt{3}$  and  $\sqrt{J_2} = \sigma_e/\sqrt{3}$ . (2.7b-c)

Solving equation (1.4) for  $\sigma_o/\sigma_e$  gives

$$\frac{\sigma_o}{\sigma_e} = \frac{\gamma}{\dot{\epsilon}_e + \gamma}. \quad (2.8)$$

Since  $1/\gamma^*$  is used more predominantly, substituting (2.8) into (2.7a) and inverting produces

$$\frac{1}{\gamma^*} = \frac{1}{\gamma} + \frac{1}{\dot{\epsilon}_e}. \quad (2.9)$$



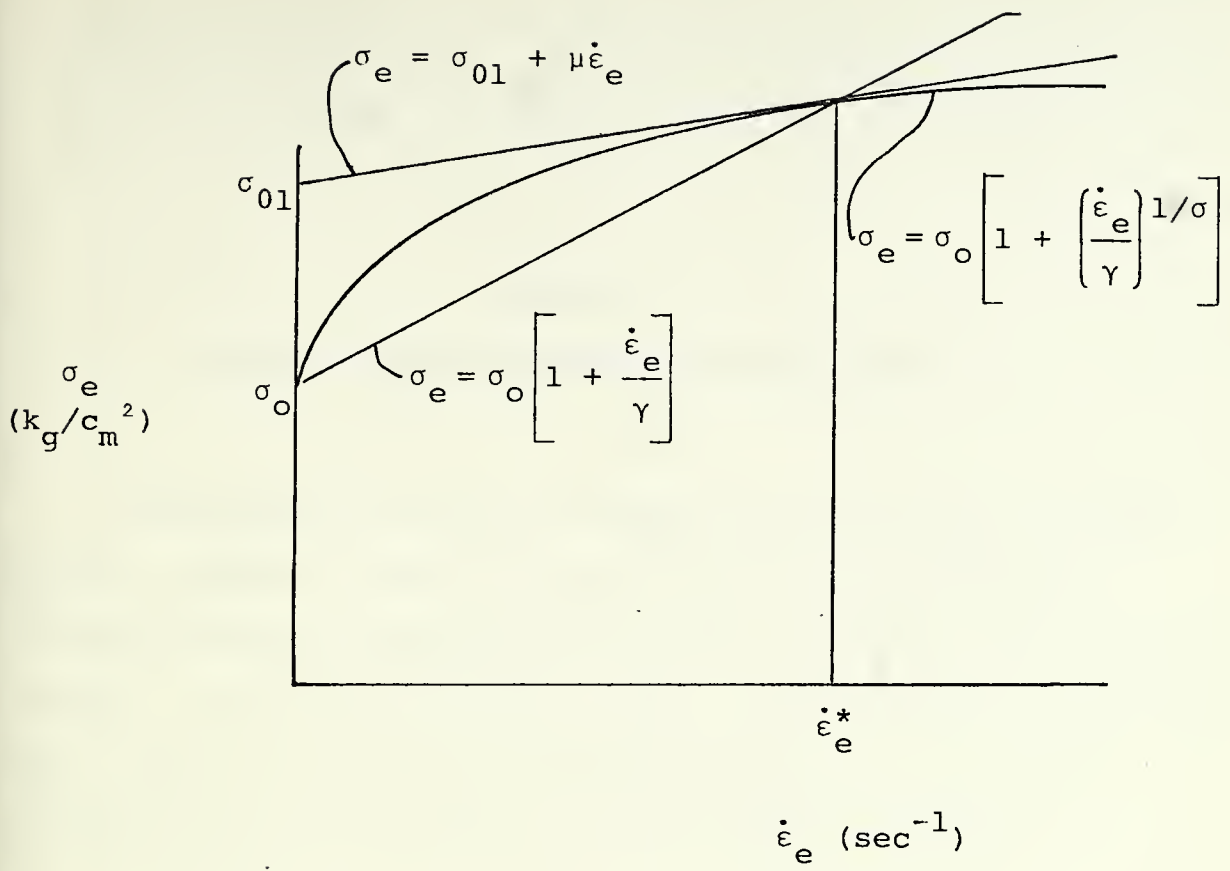


Figure 6: Cowper and Symonds Power Law and Linear Approximation to it [11].



## Appendix C

### Computer Program Using Florence Method

The following program was used to solve for  $A_{mn}(\xi)$  and  $B_{mn}(\xi)$ , equations (36a) and (36b), by use of Mathematics Library Subroutine called HYPER which is a subroutine to solve Kummer's function of the first kind. Problems were encountered when taking the difference between functions as this was eliminating the first five or six significant figures.



C MAIN PROGRAM USING FLORENCE METHOD OF SOLUTION

C INPUT VALUES

C RADIUS

C ASPECT RATIO (R/H)

C INITIAL VELOCITY

C YIELD STRESS

C VISCOSITY COEF. (GAMMA)

C DENSITY

C CCKPER/SYMCNDS PCWER CCNST

C DIMENSION APN(40), BMN(40)

C REAL \*8 A, G, RM, CLDRM, DELTA

C REAL \*8 RMZ, RMC, RMP, URNZ, URMQ, URNP, UMZ, UMO, UMP

C INTEGER\*4 N, IERR

75 REAC(5,100,ENC=99) R,RCH,VC, SIGMA, GAM, RHC, DELTA

WRITE(6,101) R,RCH,VO, SIGMA, GAM, RHC, DELTA

61 ASQ = 1./((12.\*ROH\*\*2)

RT3 = SQRT(3.0)

SIGMA1 = SIGMA\*(1.+(2./R\*VC/GAM)\*\*(1./DELTA))\*(1.-1./DELTA))

GAM1 = DELTA\*2./R\*VO\*((GAM/VO\*R/2.)\*(1./DELTA)+1.-1./DELTA)

C = SQRT(SIGMA1/RHC/RT3)

VND = R\*GAM1/VC

SOS = VND\*\*2\*(2./VND - ALOG(1.+2./VND))/RT3

TAUF = VO\*SOS/(2.\*RT3\*C)

WRITE(6,150) TAUF,SCS, C,SIGMA1,GAM1

C COMPUTATION OF ETA'S

DO 1 J=1,6

ETA = 1. - 0.2\*(J-1)

IND = 0

YMAX = 0.

C COMPUTE VALUES OF AN(ETA) AND BN(ETA)

DO 2 M=2,40

FLOR0001  
FLOR0002  
FLOR0003  
FLOR0004  
FLOR0005  
FLOR0006  
FLOR0007  
FLOR0008  
FLOR0009  
FLOR0010  
FLOR0011  
FLOR0012  
FLOR0013  
FLOR0014  
FLOR0015  
FLOR0016  
FLOR0017  
FLOR0018  
FLOR0019  
FLOR0020  
FLOR0021  
FLOR0022  
FLOR0023  
FLOR0024  
FLOR0025  
FLOR0026  
FLOR0027  
FLOR0028  
FLOR0029  
FLOR0030  
FLOR0031  
FLOR0032  
FLOR0033  
FLOR0034  
FLOR0035  
FLOR0036





```

YN = M*(M+1)
WN = 3.*(YN-2.)/(2.*YN-1.) + ASQ*(2.*YN-3.)*{YN-2.}
QN1 = TAUF*C*WN/(R*GAN1)
CN2 = TAUF*C*WN/(VO*2.)
RN2 = 1.5*TAUF**2*YN
CN = SQRT(QN1**2 + 4.*RN2)
ELN = (CN1-CN)/2.
AN = CN2*(CN1/CN - 1.)/2.
BN = QN2
AT = 1.+AN+BN
GT = 2.+BN
ZT = ON*ETA
TEST = QN2*ALOG(QN1)
IF(TEST.GT.174.) GO TO 80
MAX = N
DELTA = .000001
IF (J.EQ.6) GO TO 51

C
C
C      COMPUTE M(A,G,Z)

A = AT
G = GT
Z = ZT
IF(Z.GT.8.) GO TO 3
IF(G.GT.8.) GO TO 3
CALL HYPER(A,G,Z,RM,GLDRM,N,DELTA,IERR)
GO TO 4
3 CALL AHYP(A,G,Z,RM,OLCRM,N,DELTA,IERR)
4 IF(IERR.EQ.0) GC TO 5
5 RMZ = RM

C
C
C      COMPUTE M(1+A-G, 2-G, Z)

A = 1. + AT - GT
G = 2. - GT
Z = ZT

```



```

IF(Z.GT.8.) GO TO 6
IF(G.GT.8.) GO TO 6
CALL HYPER(A,G,Z,RM,OLCRM,N,DELTA,IERR)
GO TO 7
6 CALL AHYP(A,G,Z,RM,OLCRM,N,DELTA,IERR)
7 IF(IERR.EQ.0) GO TO 8
8 URMZ = RM

```

```

C
C COMPUTE M(A,G, OMEGA N)
C

```

```

51 A = AT
G = GT
Z = CN
IF(Z.GT.8.) GO TO 9
IF(G.GT.8.) GO TO 9
CALL HYPER(A,G,Z,RM,OLCRM,N,DELTA,IERR)
GO TO 10
9 CALL AHYP(A,G,Z,RM,CLDRM,N,DELTA,IERR)
10 IF(IERR.EQ.0) GO TO 11
11 RMC= RM

```

```

C
C COMPUTE M'(A, G, OMEGA N)= A/G*M(A+1,G+1,CN)
C

```

```

A = AT+1.
G = GT+1.
Z = ON
IF(Z.GT.8.) GO TO 12
IF(G.GT.8.) GO TO 12
CALL HYPER(A,G,Z,RM,OLCRM,N,DELTA,IERR)
GO TO 13
12 CALL AHYP(A,G,Z,RM,CLDRM,N,DELTA,IERR)
13 IF(IERR.EQ.0) GO TO 14
14 RMP = RM*AT/GT

```

```

IF(J.NE.6) GO TO 200
AMN(M) = EXP(-(ELN+ON))*((ELN+1.+BN)*RMO+ON*RMP)/(1.+BN)
BMN(N) = EXP(-(ELN+CN))*RMO/(1.+BN)*2.*TAUF

```

FLORC073  
FLOR0074  
FLOR0075  
FLORC076  
FLOR0077  
FLORC078  
FLORC079  
FLORC080  
FLOR0081  
FLORC082  
FLORC083  
FLOR0084  
FLORC085  
FLORC086  
FLOR0087  
FLORC088  
FLORC089  
FLORC090  
FLOR0091  
FLORC092  
FLORC093  
FLOR0094  
FLORC095  
FLOR0096  
FLORC097  
FLORC098  
FLORC099  
FLORC100  
FLOR0101  
FLORC102  
FLORC103  
FLOR0104  
FLOR0105  
FLOR0106  
FLOR0107  
FLOR0108



FLOR0109  
FLOR0110  
FLOR0111  
FLOR0112  
FLOR0113  
FLOR0114  
FLOR0115  
FLOR0116  
FLOR0117  
FLOR0118  
FLOR0119  
FLOR0120  
FLOR0121  
FLOR0122  
FLOR0123  
FLOR0124  
FLOR0125  
FLOR0126  
FLOR0127  
FLOR0128  
FLOR0129  
FLOR0130  
FLOR0131  
FLOR0132  
FLOR0133  
FLOR0134  
FLOR0135  
FLOR0136  
FLOR0137  
FLOR0138  
FLOR0139  
FLOR0140  
FLOR0141  
FLOR0142  
FLOR0143  
FLOR0144

```

GO TO 68
C
C  COMPUTE M(1+A-G, 2-G, OMEGA N)
C
200 A = 1.+AT-GT
    G = 2.-GT
    Z = CN
    IF(Z.GT.8.) GO TO 15
    IF(G.GT.8.) GO TO 15
    CALL HYPER(A,G,Z,RM,OLCRM,N,DELTA,IERR)
    GO TO 16
15  CALL AHYP(A,G,Z,RM,CLDRM,N,DELTA,IERR)
16  IF(IERR.EQ.0) GO TO 17
17  URMC = RM
C
C  COMPUTE M(1+A-G,1-G, OMEGA N)
C
    A = 1.+AT-GT
    G = 1.-GT
    Z = CN
    IF(Z.GT.8.) GO TO 18
    IF(G.GT.8.) GO TO 18
    CALL HYPER(A,G,Z,RM,OLCRM,N,DELTA,IERR)
    GO TO 19
18  CALL AHYP(A,G,Z,RM,CLDRM,N,DELTA,IERR)
19  IF(IERR.EQ.0) GO TO 20
20  URMP = RM
    X = 1.+AT-GT
    CALL NEGAM(X,GM)
    G1 = GM
    X = GT
    CALL NEGAM(X,GM)
    G2 = GM
    X = AT
    CALL NEGAM(X,GM)
    G3 = GM

```









68 IF (YMAX.GT.AMN(M)) GO TO 69

YMAX = AMN(M)

GO TO 2

69 IND = INC+1

IF (IND.EQ.6) GO TO 70

2 CCNTINUE

70 MAX = N

80 CONTINUE

WRITE(6,103) ETA

WRITE(6,104) (I,AMN(I),BMN(I),I=2,MAX)

1 CCNTINUE

GO TO 75

99 STOP

100 FORMAT(7F10.3)

101 FORMAT('1',4X,'R=',F12.3,' IN.', 8X,'R/H=',F9.1,15X,'VEL=',F10.3,  
1' IN/SEC',//,5X,'SIGMA=',F8.1,' PSI ', 8X,'GAMMA=',F7.1, ' SEC-1'

2,8X,'RHC=',F10.8,' LBS-SEC\*\*2/IN\*\*4',//,5X,'DELTA=',F8.1)

103 FCRMAT('0',4X,'ETA=',F10.4,6X,'N=',5X,'AN(ETA)=' ,20X,'BN(ETA)=' )

104 FORMAT(' ',24X,12,5X,E16.7,7X,E16.7)

150 FCRMAT('0 TAU=',F17.7,5X,'SOS=',E16.7,7X,'C=' ,E16.7,//,5X,

1'SIGMA1=',E15.7,' GAM1=',E15.7)

END

1

60

1

FLOR0181  
FLOR0182  
FLCR0183  
FLOR0184  
FLORC185  
FLCR0186  
FLOR0187  
FLOR0188  
FLOR0189  
FLCR0190  
FLOR0191  
FLOR0192  
FLOR0193  
FLOR0194  
FLOR0195  
FLCR0196  
FLOR0197  
FLOR0198  
FLOR0199  
FLOR0200  
FLOR0201  
FLOR0202



C SUBROUTINE TO COMPUTE KUMMER FUNC IN ASYMPTOTIC EXPANSION

C

SUBROUTINE AHYP(A, G, Z, RM, CLDRM, N, DELTA, IERR)

REAL \*8 A, G, RM, CLDRM, DELTA, TERM, TERM1, CVL, VL

IERR = 0

AS = 1.-A

GS = G-A

VL = 1.

TERM = 1.

AT2 = 1000000.

DO 5 N=1,130

TERM1 = (AS+N-1.)\*(GS+N-1.)/(N\*Z)

6 TERM = TERM\*TERM1

AT1 = DABS(TERM)

AB = AS+N-1.

GB = GS+N-1.

C

TEST IF AB OR GB ARE NEGATIVE

C

C

IF(AB.LT.0.) GC TC 4

I

IF(GB.LT.0.) GC TO 4

C

TEST IF ABSCLUTE VALUE OF NEW TERM IS GREATER THAN LAST TERM

C

C

IF(AT1.GT.AT2) GO TO 7

4 AT2 = AT1

OVL = VL

VL = OVL + TERM

ERR = DABS(1. - OVL/VL)

IF(ERR.LE.DELTA) GC TO 8

5 CONTINUE

GC TO 8

7 N = N-1

IERR = 3

8 IF(N.EQ.130) IERR = 5

X = G

AHYP0001  
AHYP0002  
AHYP0003  
AHYP0004  
AHYP0005  
AHYP0006  
AHYP0007  
AHYP0008  
AHYP0009  
AHYP0010  
AHYP0011  
AHYP0012  
AHYP0013  
AHYP0014  
AHYP0015  
AHYP0016  
AHYP0017  
AHYP0018  
AHYP0019  
AHYP0020  
AHYP0021  
AHYP0022  
AHYP0023  
AHYP0024  
AHYP0025  
AHYP0026  
AHYP0027  
AHYP0028  
AHYP0029  
AHYP0030  
AHYP0031  
AHYP0032  
AHYP0033  
AHYP0034  
AHYP0035  
AHYP0036



```

CALL NEGAM(X,GM)
GG = GM
X = A
CALL NEGAM(X,GM)
GA = GM
T1 = GG/GA#Z**(A-G)#EXP(Z)
OLDRM = T1*CVL
RM = T1*VL
RETURN
END

```

```

AHYP0037
AHYP0038
AHYP0039
AHYP0040
AHYP0041
AHYP0042
AHYP0043
AHYP0044
AHYP0045
AHYP0046

```



C SUBROUTINE TO COMPUTE GAMMA FUNC WITH POSSIBLE NEGATIVE VALUES OF ARG.

C

```

SUBROUTINE NEGAM(X,GM)
  GA = 0.
  XT = -X
  IF(XT.GT.55) GO TO 200
  DO 5 J=1,50
  IF(XT.LT.0.) GO TO 100
  GA = GA - ALOG(XT)
  XT = XT - 1.
  5 CONTINUE
100 N = J - 1
  GN = ALGAMA(-XT) + GA
  GM = (-1)**N*EXP(GN)
  RETURN
200 GM = 0.
  RETURN
  END

```

NGAM0001  
 NGAM0002  
 NGAM0003  
 NGAM0004  
 NGAM0005  
 NGAM0006  
 NGAM0007  
 NGAMC008  
 NGAM0009  
 NGAM0010  
 NGAMC011  
 NGAM0012  
 NGAM0013  
 NGAMC014  
 NGAM0015  
 NGAM0016  
 NGAMC017  
 NGAMC018





## Appendix D

### Computer Program Using Numerical Method

The following program solved the basic equation (34a) for  $A_{mn}(\xi)$  and  $B_{mn}(\xi)$  by use of Mathematics Library Subroutine called DQSYK which is a subroutine to solve up to fourth order simultaneous differential equations with initial conditions. This program used equation (34d).



C PROGRAM TC SOLVE SECCND CRDR DIFFERENTIAL EQUATION

C INPUT VALUES

C RADIUS

C ASPECT RATIO (R/H)

C INITIAL VELCCITY

C YIELD STRESS

C VISCOSITY COEF. (GAMMA)

C DENSITY

C CONSTANT (FLORENCE SOLN) /

C COWPER/SYMONDS POWER

C DELTA

INTEGER\*4 N,KDEG(1),IFLAG,MXSTEP,KSTEP,KERMAX,KORDER(1)  
 REAL\*4 EPS(1),HMIN,HMAX,ERRMAX,AMN(6,50),BMN(6,50)  
 REAL\*8 T,Y(2),F(1),H,DEL,TFINAL,YSAVE(2),DIABLE(17,1)  
 DATA N,KDEG(1),EPS(1),H,HMIN,HMAX,DEL,TFINAL,MXSTEP,KORDER(1)/1,  
 \*2,.C00C1,-.05,.C01,.1,-.2,.C0C01,25,6/  
 75 READ(5,100,END=99) R,ROH,VO, SIGMA, GAM, RHO, CONST, DELTA

WRITE(6,101) R,RCH,VC, SIGMA, GAM, RHO, CONST,DELTA

61 ASQ = 1./((12.\*RCH\*\*2)

RT3 = SQR(3.0)

SIGMA1 = SIGMA\*(1.+(2./R\*VC/GAM)\*\*(1./DELTA)\*(1.-1./DELTA)).

GAM1 = DELTA\*2./R\*VC\*((GAM/VO\*R/2.)\*(1./DELTA)+1.-1./DELTA)

C = SQR((SIGMA1/RHO/RT3)

VND = R\*GAM1/VO

SOS = VND\*\*2\*(2./VND - ALOG(1.+2./VND))/RT3

TAUF = VO\*SOS/(2.\*RT3\*C)

WRITE(6,150) TAUFSOS, C,SIGMA1,GAM1

IND=0

MAX = 1

YMAX = 0.

DO 2 M=2,40

YN = M\*(M+1)

WN = 3.\*(YN-2.)/(2.\*YN-1.) + ASQ\*(2.\*YN-3.)\*(YN-2.)

QN1 = TAUFC\*WN/(R\*GAM1)

QN2 = TAUFC\*WN/(VO\*2.)

RN2 = TAUFC\*\*2\*YN

NUM10001  
 NUM10002  
 NUM10003  
 NUM10004  
 NUM10005  
 NUM10006  
 NUM10007  
 NUM10008  
 NUM10009  
 NUM10010  
 NUM10011  
 NUM10012  
 NUM10013  
 NUM10014  
 NUM10015  
 NUM10016  
 NUM10017  
 NUM10018  
 NUM10019  
 NUM10020  
 NUM10021  
 NUM10022  
 NUM10023  
 NUM10024  
 NUM10025  
 NUM10026  
 NUM10027  
 NUM10028  
 NUM10029  
 NUM10030  
 NUM10031  
 NUM10032  
 NUM10033  
 NUM10034  
 NUM10035  
 NUM10036



```

T = 1.
Y(1) = 1.
Y(2) = 0.
J = 0
CALL DQSYK(N,T,Y,F,KDEG,EPS,IFLAG,H,HMIN,HMAX,DELT,TFINAL,MXSTEP,
1KSTEP,KERMAX,ERRMAX,KORDER,YSAVE,DTABLE)
GO TO 20
10 CALL DQSYK1
20 GO TO(22,22,23,24,25,26,27,28),IFLAG
22 F(1) = (QN1 + CN2/T)*Y(2) + RN2*Y(1)*(1.5+3.*VO*T/R/GAM1)
GO TO 10
23 J = J + 1
AMN(J,M) = Y(1)
GO TO 10
24 AMN(6,M) = Y(1)
IF(YMAX.GT.Y(1)) GO TO 31
YMAX = Y(1)
GO TO 30
31 IND=IND+1
IF(IND.EQ.6) MAX=M
GO TO 30
25 GO TO 10
26 EPS(1) = 32.*ERRMAX*EPS(1)
GO TO 10
27 HMIN = DABS(H)
GO TO 10
28 WRITE(6,190)
STCP
30 CONTINUE
T = 1.
Y(1) = 0.
Y(2) = -2.*TAUF
J = 0
CALL DQSYK(N,T,Y,F,KDEG,EPS,IFLAG,H,HMIN,HMAX,DELT,TFINAL,MXSTEP,
1KSTEP,KERMAX,ERRMAX,KORDER,YSAVE,DTABLE)
35 CALL DQSYK1

```

NUM10037  
 NUM10038  
 NUM10039  
 NUM10040  
 NUM10041  
 NUM10042  
 NUM10043  
 NUM10044  
 NUM10045  
 NUM10046  
 NUM10047  
 NUM10048  
 NUM10049  
 NUM10050  
 NUM10051  
 NUM10052  
 NUM10053  
 NUM10054  
 NUM10055  
 NUM10056  
 NUM10057  
 NUM10058  
 NUM10059  
 NUM10060  
 NUM10061  
 NUM10062  
 NUM10063  
 NUM10064  
 NUM10065  
 NUM10066  
 NUM10067  
 NUM10068  
 NUM10069  
 NUM10070  
 NUM10071  
 NUM10072



```

GO TO 40
40 GC TC(42,43,44,45,46,47,48), IFLAG
42 F(1) = (QN1 + QN2/T)*Y(2) + RN2*Y(1)*(1.5+3.*VO*T/R/GAM1)
GO TO 35
43 J = J + 1
   BMN(J,M) = Y(1)
GO TO 35
44 BMN(6,M) = Y(1)
   IF(MAX.EQ.M) GC TC 49
GO TO 2
45 GO TO 35
46 EPS(1) = 32.*ERRMAX*EPS(1)
GO TO 35
47 HMIN = DABS(H)
GO TO 35
48 WRITE(6,190)
   STOP
   2 CCNTINUE
49 DO 50 KC=1,6
   ETA = 1. - 0.2*(KC-1)
   WRITE(6,103) ETA
   WRITE(6,176)(I,AMN(KO,I),BMN(KO,I),I=2,MAX)
50 CONTINUE
GO TO 75
99 STOP
100 FORMAT(8F10.3)
101 FORMAT('1',4X,'R=',F10.3,' IN.',10X,'R/H=',F8.3,15X,'VEL=',F10.3,
1' IN/SEC',//,5X,'SIGMA=',F7.0,' PSI', 9X,'GAMMA=',F6.0,' SEC-1',
2,8X,'RHC=',F10.8,' LBS-SEC**2/IN**4',//,5X,'CONST=',F6.2,15X,
3'DELTA=',F3.1)
103 FORMAT('0',4X,'ETA=',F10.4,6X,'N=',5X,'AN(ETA)=' ,20X,'BN(ETA)=' )
150 FORMAT('0'  TAUF=',E16.7,' SOS=',E16.7,' C=' ,E16.7,/,5X,
1'SIGMA1=',E16.7,' GAM1=',E16.7)
176 FORMAT(' ',24X,I2,5X,E16.7,7X,E16.7)
190 FORMAT('0 IFLAG = 8')
END

```





## Appendix E

### Critical Impulse

It is straightforward to show when  $\lambda_n \gg 1$  that  $\lambda_n$  can be eliminated from equations (34c) and (34e) and using equation (24b) to give

$$\frac{\rho V_o^2}{\sigma_o} = \frac{8}{\sqrt{3}} \frac{R_n^2}{(\sigma_o/\sigma_e)^2} \frac{h/R}{\left\{ \frac{24\sqrt{3} Q_n^{(2)}}{(\sigma_o/\sigma_e)} - 9 \right\}^{1/2}} \quad (5.1)$$

where  $\sigma_o/\sigma_e$  is defined in equation (30). As shown in Table 4 the values of  $\sigma_o/\sigma_e$  lie within the range  $0.98 < \sigma_o/\sigma_e < 1.16$  with a medium value  $\sigma_o/\sigma_e \approx 1.07$ . Also the values of  $Q_n^{(2)}$  lie within the range  $1.27 < Q_n^{(2)} < 4.42$  with a medium value of 2.84. It is straightforward to show when using equation (34c) with  $n \gg 1$ , that the critical harmonic

$$n = 3.173(R/h)^{1/2} \quad (5.2)$$

is associated with these values of  $\sigma_o/\sigma_e$  and  $Q_n^{(2)}$ .

The threshold of dynamic plastic instability could be said to occur when  $A_{mn}(0) = X$ , where  $X$  is an arbitrary positive number. If  $X = 100$ , then the initial displacement imperfections in the critical mode are magnified by a factor of one hundred. This amplification is achieved when  $R_n \approx 1.7$  according to Florence [3] asymptotic formula for equation (36a)



$$A_{mn}(0) = \exp \left[ -(\Lambda_n + \Omega_n) \right] \left\{ \frac{(\Lambda_n + 1 + b_n) M(\Omega_n) + \Omega_n M'(\Omega_n)}{1 + b_n} \right\} \quad (5.3)^*$$

where the right hand quantities are defined in equations (37a-h).

$V_o$ ( $10^3$ in/sec)	$\gamma$ ( $\text{sec}^{-1}$ )	$\sigma_o/\sigma_e$	Critical Harmonic	$Q_n^{(2)}$
5	40	1.00	11	1.27
30	40	0.98	13	2.23
5	6500	1.06	11	1.35
30	6500	1.03	15	3.99
5	1,288,000	1.11	11	1.41
25	1,288,000	1.10	15	4.26
5	900,000,000	1.16	11	1.47
22.5	900,000,000	1.14	15	4.42

Table 4: Variation of  $\sigma_o/\sigma_e$  and  $Q_n^{(2)}$  to various values of  $\gamma$  with  $R = 1.460$  in.,  $R/h = 18.25$   $\sigma_o = 46,000$  psi and  $\rho = 0.0002523$  lb-sec<sup>2</sup>/in.<sup>4</sup>.

Finally equation (5.1) predicts a non-dimensionalized critical or threshold velocity

$$\frac{\rho V_o^2}{\sigma_o} = 1.11 h/R \quad (5.4)$$

\* This asymptotic formula gave agreement with numerical values at  $\xi = 0$  up to 4 significant figures.



This value does not compare favorably with Jones' [13] in which his coefficient is 17.8, since the velocities required should be higher than in the rigid-plastic case.



Thesis  
D553

Dickey

Dynamic buckling of  
viscoplastic spherical  
shells.

153108

27 SEP 74

DISPLAY

Thesis  
D553

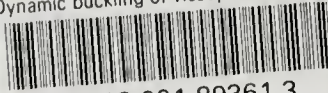
Dickey

Dynamic buckling of  
viscoplastic spherical  
shells.

153108

thesD553

Dynamic buckling of viscoplastic spheric



3 2768 001 89361 3

DUDLEY KNOX LIBRARY